Table 1. Summary of the genetic and epigenetic abnormalities in ATLL cell lines

Cell line	Cell type	10p abnormalities	Point mutation	Treatment		
				5-Aza-dC, fold ± SD	TSA, fold ± SD	5-Aza-dC+TSA, fold ± SD
MOLT4	T-ALL	None	None	1.25 ± 0.46	1.65 ± 0.21	1.65 ± 0.22
Jurkat	T-ALL	None	None	11.17 ± 0.59*	10.04 ± 1.74*	3.07 ± 0.54*
MT2	HTLV-1 (+)	None	None	3.38 ± 1.17*	8.25 ± 1.76*	4.58 ± 0.90*
HUT102	HTLV-1 (+)	None	255A>C Asn78Thr	4.39 ± 0.49*	6.94 ± 0.16*	8.03 ± 1.05*
ED	ATLL	None	None	4.32 ± 1.57*	7.48 ± 0.91*	3.93 ± 0.21*
KOB	ATLL	10p del	None	3.26 ± 1.12*	2.32 ± 0.81	2.08 ± 0.54
KK1	ATLL	10p del	None	9.92 ± 0.45*	6.76 ± 0.17*	9.72 ± 0.35*
SO4	ATLL	10p del	None	1.40 ± 0.33	1.57 ± 0.18	0.59 ± 0.06
S1T	ATLL	None	None	3.66 ± 0.21*	3.95 ± 0.75*	2.32 ± 1.63
Su9T	ATLL	None	None	3.91 ± 0.45*	9.66 ± 2.38*	1.42 ± 0.21

Data are means plus or minus SD.
*$P < .05$ versus control (Dunnett test).

signals were detected in the 1-Mb region from RP11-135A24 to RP11-462L8 in ATL090, suggesting that a 10p11 region-specific homozygous deletion had occurred in this case (Figure 1B). Therefore, a minimal common region of chromosome deletions, including a region of homozygous deletion in ATL090, was mapped to a 2-Mb region from PR11-523J14 to RP11-342D11 (Figure 1B).

To confirm these results, we performed SNP array-CGH using DNA from 8 ATLL-related cell lines including KK1, KOB, SO4, and an additional 10 samples from acute-type ATLL patients. Deletions in 10p11.2, including the 2-Mb deletion region, were noted in 3 cell lines: KK1, KOB, and SO4, and an additional 4 patient samples (Figure 1B; Table S3). Using SNP array-CGH, the telomeric deleted regions in chromosome 10p11.2 in KOB and KK1 covered a wider area than those detected by FISH analysis, and each deleted region in the 3 cell lines and 4 patients samples covered the common deletion region. To combine these data, the same minimal common region of chromosome deletions, including regions of homozygous deletion in ATL090, was mapped to a 2-Mb region from PR11-523J14 to RP11-342D11 (Figure 1B), suggesting that a tumor suppressor gene possibly exists in this 2-Mb region in 10p11.2.

Down-regulation of *TCF8* mRNA in ATLL cells

We examined the mRNA expression profiles of all 12 genes within the commonly deleted region in 10p11.2, which were identified by NCBI and Celera gene maps (Rockville, MD). Since mRNA samples from the ATLL patients used for the deletion mapping were not available, we initially used the mRNA expression profiles of the other 8 leukemia cell samples from acute-type ATLL patients by semiquantitative reverse-transcription PCR (RT-PCR), which had been previously identified by DNA microarray.[15] Two leukemia samples from patients with ATLL had chromosome 10p11.2 abnormalities: t(10;15) (p11.2;q26) in ATL044 and monosomy 10 in ATL009 (Table S1). Expression levels of 8 genes (*TCF8, ARHGAP12, KIF5B, CCDC7, EPC1, C10orf68, ITGB1* and *NRP1*) and HTLV-1 *Tax* as well as *β-actin* are shown in Figure 2A. The results showed that levels of *TCF8* mRNA in ATLL cells had a tendency to be lower than those in $CD4^+$ T lymphocytes from healthy volunteers, even though only 2 of 8 patients had chromosome 10p11.2 abnormalities. Other genes did not show any differences in expression level between the 2 groups. Expression profiles of the leukemia cells using a DNA microarray gave the same results (Figure S1), and quantitative real-time RT-PCR also showed that the expression level of *TCF8* mRNA in ATLL cells was significantly lower than that in $CD4^+$ T lymphocytes (Figure 2B).

To confirm these results, 12 T-ALL cell lines containing 6 ATLL cell lines (ED, KOB, KK1, SO4, S1T, and Su9T), 2 HTLV-1–infected T-cell lines (MT2 and HUT102), and 4 HTLV-1–uninfected T-ALL cell lines (Jurkat, MOLT4, MKB1, and KAWAI) were used for an expression study. Three cell lines (KOB, KK1, and SO4) revealed the deletion of chromosome 10p11.2 with *TCF8*. Although no other genes except *TCF8* showed any change in expression level in these cell lines (Figure S2), the expression level of *TCF8* was specifically down-regulated in all of the ATLL cell lines along with Jurkat cells by quantitative real-time RT-PCR (Figure 2C). These data suggest that *TCF8* transcription might be down-regulated by epigenetic inactivation in most ATLL-related cell lines with Jurkat cells.

Increased expression of *TCF8* by 5-aza-2′-deoxycytidine or trichostatin A in ATLL cell lines

To clarify whether DNA methylation and/or histone deacetylation of the *TCF8* gene promoter were involved in the transcriptional repression of *TCF8* in ATLL cell lines with Jurkat cells, 10 cell lines (2 T-ALL, 2 HTLV-1–infected, and 6 ATLL-derived cell lines) were cultured with (1) 10 μM 5-aza-2′-deoxycytidine (5-aza-dC), a DNA demethylating agent, for 72 hours, (2) 1.2 μM trichostatin A (TSA), an inhibitor of histone deacetylase, for 48 hours, or (3) 1.2 μM TSA for 48 hours following culture with 10 μM 5-aza-dC for 24 hours. After treatment with 5-aza-dC, *TCF8* expression was up-regulated in 8 of 10 cell lines (Jurkat, MT2, HUT102, ED, KOB, KK1, S1T, and Su9T), with more than 3-fold activation ($P < .05$) as detected by real-time RT-PCR (Table 1). After treatment with TSA for 48 hours, the levels of *TCF8* mRNA increased in 7 of 10 cell lines (Jurkat, MT2, HUT102, ED, KK1, S1T, and Su9T), also with more than 3-fold activation ($P < .05$). In addition, combination therapy induced *TCF8* mRNA expression in 5 cell lines by more than 3-fold. Therefore, *TCF8* mRNA expression was activated in 7 of 8 ATLL-related cell lines along with Jurkat cells by either 5-aza-dC or TSA treatment, suggesting that the down-regulation of *TCF8* in most of the ATLL cell lines except SO4 cells with a chromosome 10p hemizygous deletion was dependent on epigenetic abnormalities.

Unmethylated putative *TCF8* promoter in ATLL cell lines

Next, we determined the methylation status of the *TCF8* promoter by bisulfite sequencing. A CpG island containing 50 CpGs was

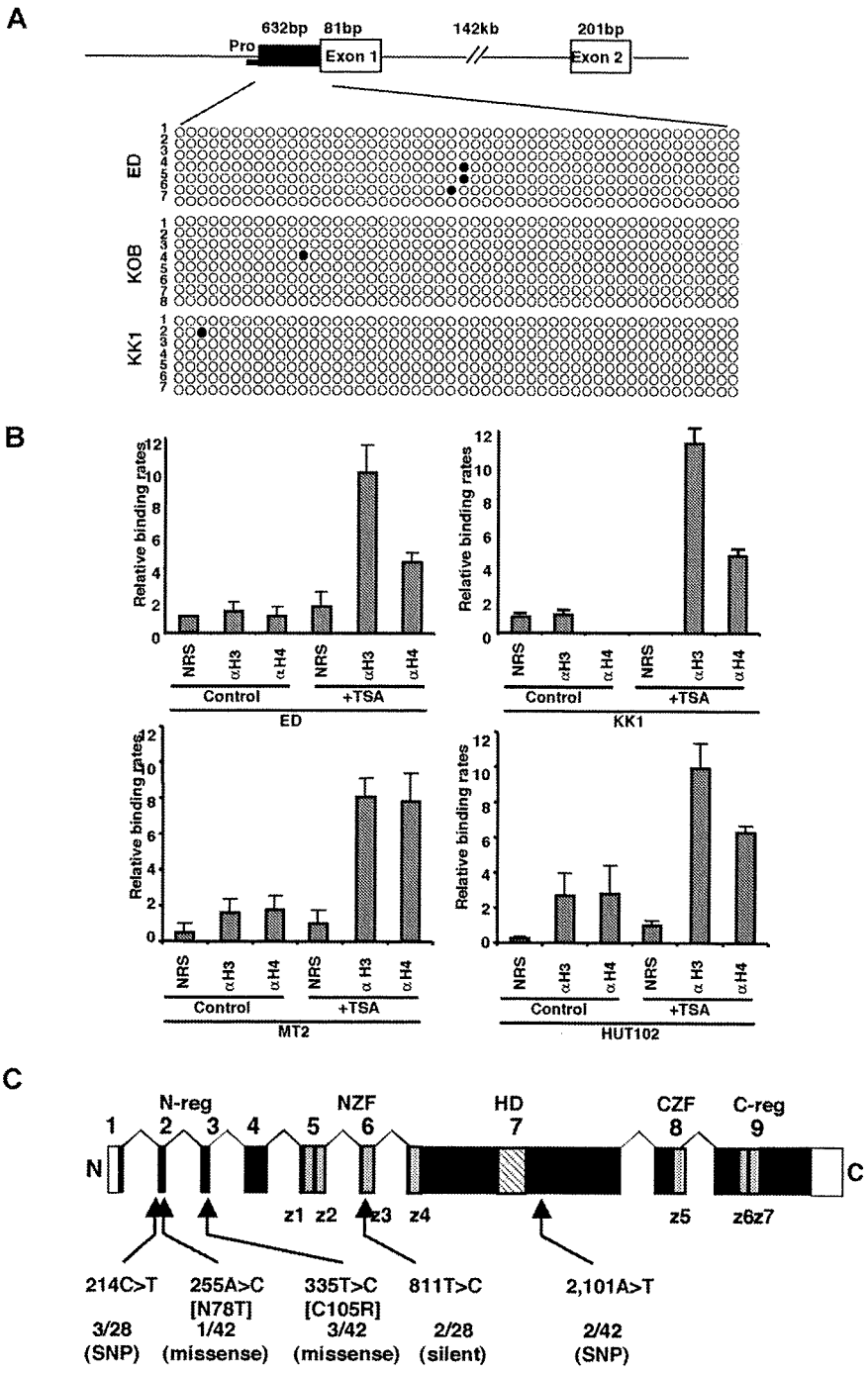

Figure 3. Genetic and epigenetic abnormalities of the *TCF8* gene in ATLL cells. (A) Bisulfite genomic sequencing of the *TCF8* promoter region in 3 ATLL cell lines: ED, KOB, and KK1. PCR products amplified from bisulfite-treated DNA were subcloned, and 8 clones in each cell line were sequenced. ○ indicate unmethylated CpGs (Thy), and ● indicate methylated CpGs (Cyt). The sequenced region contains 50 CpGs in 632 bp, just upstream from exon 1. Pro indicates a region of the *TCF8* promoter for chromatin immunoprecipitation. (B) Specific DNA binding of acetylated histone H3 or H4 to the *TCF8* promoter region detected by chromatin immunoprecipitation (ChIP). Two genomic DNA fragments containing every possible DNA-binding site, *TCF8* promoter, or *β-actin* promoter were amplified from the genomic DNA of fixed ATLL-related cell lines (MT2, HUT102, ED, and KK1) after immunoprecipitation with normal rabbit serum (NRS) or with antiacetylated histone H3 or H4 antibodies (αH3 or αH4). Quantitative PCR data calibrated to the *TCF8* promoter/*β-actin* ratio are shown in the NRS as a relative expression rate of 1. Data are the means plus or minus standard deviation of $2^{-\Delta\Delta Ct}$ in a duplicate assay. Cell lines were cultured in RPMI1640 medium containing 10% FCS with (+ TSA) or without (control) 1.2 μM TSA. (C) Genomic structure of the *TCF8* gene with a missense mutation and single nucleotide polymorphisms. Locations of the mutations and the single nucleotide polymorphisms relative to the exons encoding the functional domains are shown. *TCF8* encodes a homeodomain (HD) flanked by 2 zinc-finger clusters (z1 to z4 and z5 to z7) (NZF indicates N-terminal zinc finger repeats, CZF; C-terminal zinc finger repeats). The N-terminal transcriptional regulatory domain (N-reg) could bind to p300/CBP and the C-terminal transcriptional regulator domain (C-reg) is the region where acidic amino acids are clustered just after the last zinc-finger domain. Values represent the number of mutated cases per total number of tested cases. SNP indicates single nucleotide polymorphism. White boxes represent noncoding regions in exons 1 and 9.

amplified from a 632-bp region of the putative *TCF8* promoter adjacent to exon 1 using 2 pairs of PCR primers and bisulfite-treated genomic DNA from 3 ATLL cell lines: ED, KOB, and KK1. However, the *TCF8* promoter was not methylated in any of the 3 ATLL cell lines in which *TCF8* expression was induced by 5-aza-dC (Figure 3A), suggesting that the CpG island was not a direct target for DNA methylation in ATLL cells. Moreover, *TCF8* mRNA was up-regulated in various ATLL cell lines after treatment with hydralazine, which was reported to decrease DNA methyltransferase expression (Figure S3). This observation suggests that a transactivating regulator of *TCF8* may be modulated by methylation or the other regulatory elements are located outside the *TCF8* promoter. Such enhancer-related methylation events have been described for the imprinting of *H19* and *Igf2, p21WAF1* regulation by *p73*, and *Apaf-1*.[30-33] Therefore, further analyses will be needed to determine the exact regulatory element near the *TCF8* gene or to find a transactivating regulator of *TCF8*, which is directly methylated in ATLL cells.

Histone deacetylation is directly involved in down-regulation of *TCF8* mRNA expression in ATLL cells

To confirm the correlation between reduced *TCF8* mRNA expression and histone deacetylation, *TCF8* expression and histone acetylation status were analyzed in the ATLL-related cell lines (MT2, HUT102, ED, and KK1) by chromatin immunoprecipitation (ChIP) after treatment with or without TSA. After treatment with TSA for 48 hours, the chromosomal DNA precipitated by antiacetylated histone H3 or H4

antibody was amplified with 2 sets of primers for the *TCF8* promoter region or for the human *β-actin* promoter region (Figure 3B). Band intensities of the *TCF8* promoter region in 4 cell lines were amplified 3- to 6-fold after treatment with TSA, indicating that histone deacetylation of the *TCF8* promoter region was directly involved in the down-regulation of *TCF8* mRNA expression in ATLL cells.

Identification of missense mutations in *TCF8* in ATLL cells

We then searched for somatic *TCF8* mutations in DNA samples from 34 patients with acute-type ATLL and 10 T-cell leukemia cell lines. Genomic PCR did not detect any homozygous deletions in any of the 9 coding exons of *TCF8* in these samples. We detected 5 types of nucleotide substitutions, and all were heterozygous (Figure 3C). The 255A>C substitution in HUT102, creating a missense mutation (Asn78Thr) in exon 2, and the 335T>C substitution in the leukemia cells from 3 ATLL patients, creating a missense mutation (Cys105Arg) in exon 3, were likely to be somatic mutations (Table S4), since they were not detected in noncancerous cells from 95 Japanese volunteers.

The results of genomic and expression analysis indicate that the *TCF8* gene is altered by several mechanisms, including hemizygous deletion, epigenetic dysregulation, and intragenic mutations. Regarding the ATLL-related cell lines, 3 of 9 showed hemizygous deletions of 10p11.2; 8 of 9 showed epigenetic dysregulation of the *TCF8* gene; and 1 of 9 showed an intragenic mutation (Table 1). Therefore, *TCF8* is a strong candidate tumor suppressor gene for ATLL leukemogenesis and is initially inactivated by unbalanced translocations with heterozygous deletion in the 10p11.2 region in ATLL cells.

Development of CD4+ T-cell lymphoma in *TCF8* mutant mice

To determine whether down-regulation of the *TCF8* gene could be a causative event for leukemogenic conversion of T lymphocytes to leukemia-lymphoma cells, we investigated *δEF1* (mouse homologue of *TCF8*) gene-targeted mutant mice, which lack the COOH-proximal zinc finger clusters ($\delta EF1^{\Delta C\text{-}fin}$ allele) and were reported to have a defect in the thymic T-cell development.[28,29] Since 20% of the homozygous *TCF8* mutant mice were born alive, we made their genetic backgrounds more heterogeneous by crossing the C57BL/6 background with the ICR or F1 (C57BL/6 × C3H) mice. Homozygous mice on a mixed genetic background were born with almost normal Mendelian frequencies (wild-type: heterozygote:homozygote = 60:91:42). After 4 months, almost half of the *TCF8* homozygous mutant mice experienced enlargement of the abdomen due to ascites (27 [64.3%] of 42 mice), and many mice developed lymphomas with a median onset of disease of 30 weeks after birth and an earliest onset at 95 days after birth (Figure 4A). Half of the mice died within a year, and 84% of them developed fatal T-cell lymphomas. In *TCF8* homozygous mutant mice, 2 types of lymphomas were observed: (1) peripheral lymphomas with or without ascites, and (2) thymic tumors. Typical pathological findings of 15 mice (no. 6 to no. 21) are shown in Table S5. In the peripheral lymphoma group, a large amount of bloody or milky ascitic fluid had collected in approximately 60% of the mice with invasion of various organs (Figure 4B,C). Numerous lymphoma cells with medium to large, cleaved or noncleaved nuclei were observed in the ascitic fluid (Figure 4D). Lymphoma cells had invaded various lymph nodes, including the thoracic, peripancreatic, mesenteric, perirenal, mesenteric, and other peripheral lymph nodes (Figure 4E). Fluorescence-activated cell sorter

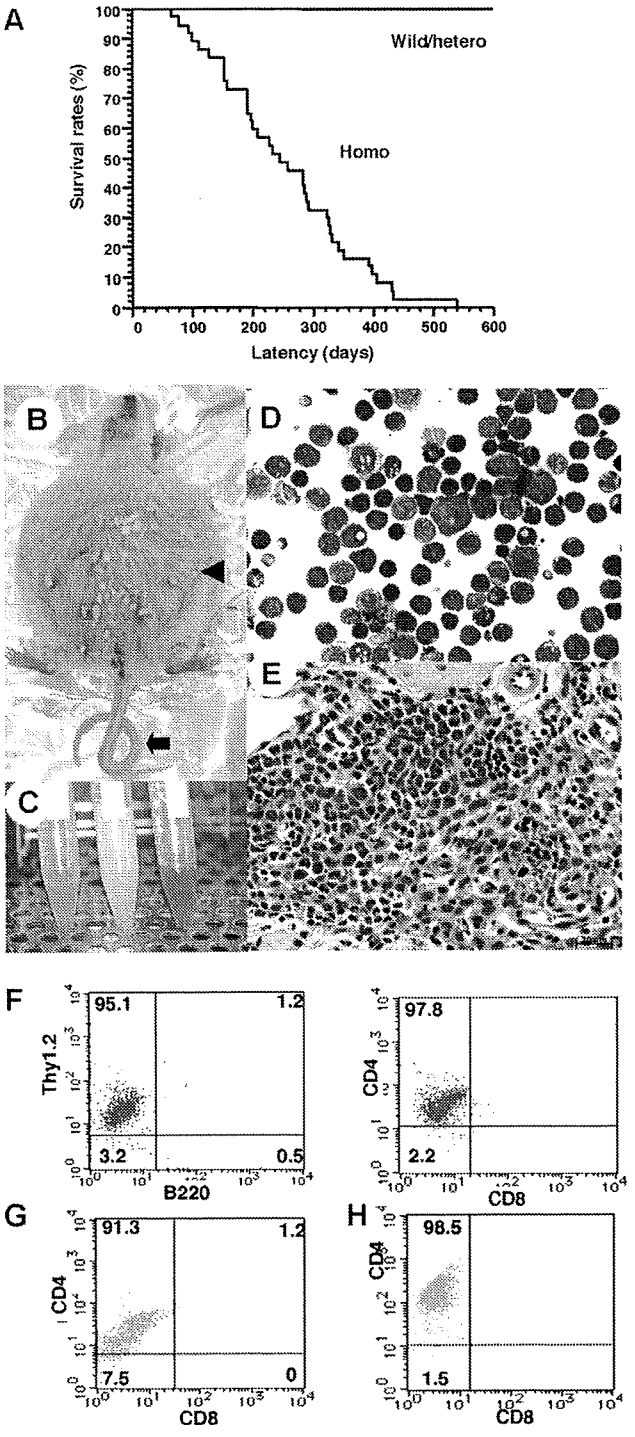

Figure 4. Survival rates and pathologic findings in *TCF8* mutant mice. (A) The survival rates of a cohort of wild-type (wild), *TCF8* heterozygous (hetero), and *TCF8* homozygous (homo) mutant mice were followed over the indicated period using Kaplan-Meier plots. (B) Gross photograph of *TCF8* mutant mice with ascites (◀). Approximately 30% of *TCF8*-homologous mutant mice showed curled tail (◆). (C) Bloody or milky ascites was pooled. (D) May-Giemsa staining of tumor cells in ascites. Original magnification ×400. (E) Many lymphoma cells with medium- to large-sized nuclei infiltrated in the mesentery. Cells were examined using an Axioskop 2 plus inverted microscope (Carl Zeiss, Rugby, United Kingdom) and digital images were aquired using AxioCam camera and AxioVision 2.05 software (Carl Zeiss). Original magnification ×400. (F) Tumor cells from ascitic fluids were analyzed by staining with a combination of monoclonal antibodies, either Thy1.2-PE with B220-FITC (left) or CD4-PE with CD8-FITC (right) and FACS. (G,H) The tumor cells that invaded liver (G) or spleen (H) were analyzed by staining with a combination of monoclonal antibodies, CD4-PE with CD8-FITC.

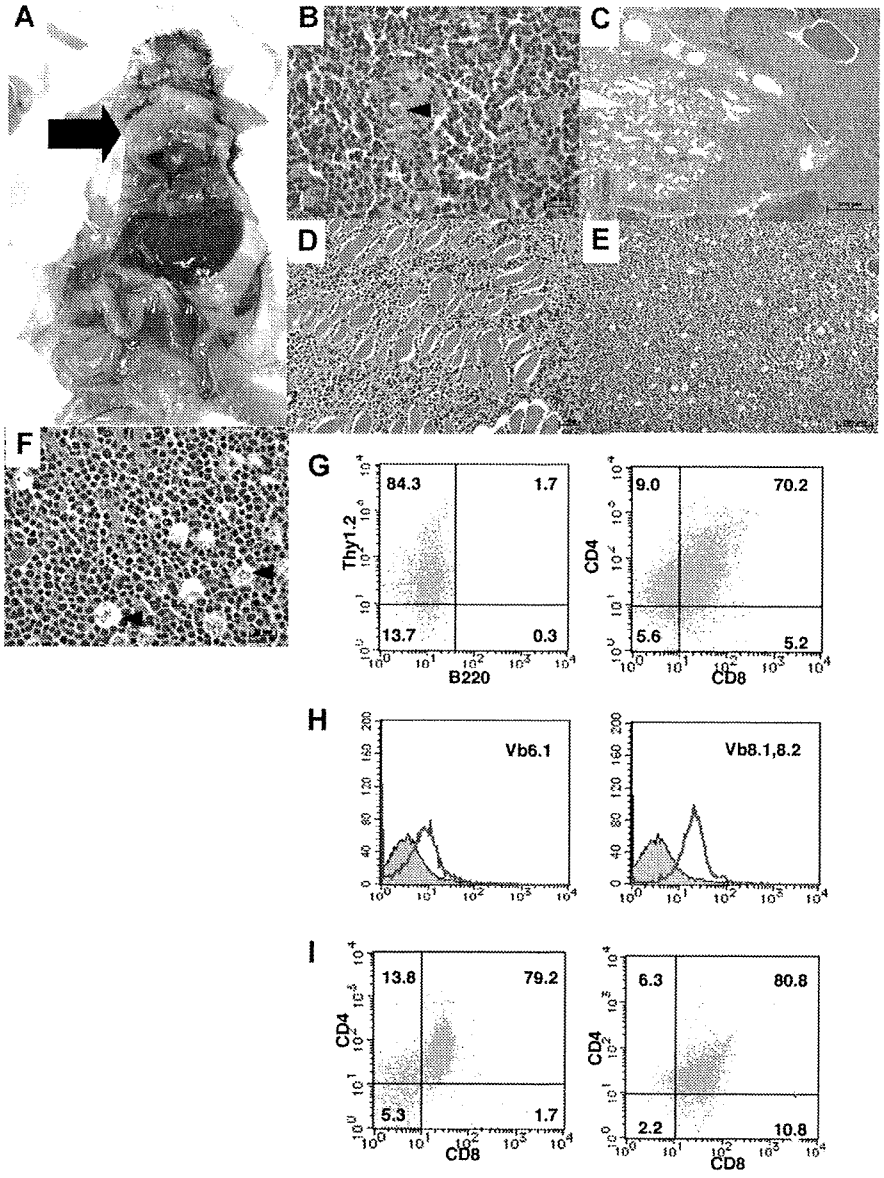

Figure 5. Pathological findings of *TCF8* mutant mice. (A) Gross autopsy of *TCF8* mutant mice with thymic tumors. A large thymic tumor (➔) was observed at the mediastinum of the dissected mouse. (B) Hematoxylin and eosin staining of tumor sections from the mouse as indicated. The normal thymic cellular architecture in the *TCF8* mutant mice is replaced with monotonous fields of large, highly mitotic lymphoblasts with small Hassall bodies (◀). The scale bar indicates 20 μm. Original magnification ×400. (C) The tumor cells invaded the lung, vascular tissues, and heart in the mouse. The scale bar indicates 500 μm. Original magnification ×25. (D) The tumor cells invaded the muscular tissues of the chest wall. The scale bar indicates 50 μm. Original magnification ×200. (E) Hematoxylin and eosin staining of peripheral lymph nodes. Tumor cells showed a diffuse proliferation of monomorphic lymphoma cells, focally mixed with tingible body macrophages ("starry-sky appearance") (◀). The scale bar indicates 100 μm. Original magnification ×100. (F) Hematoxylin and eosin staining of peripheral lymph nodes. The scale bar indicates 20 μm. Original magnification ×400. (G) Tumor cells from the thymic tumor were analyzed by staining with a combination of monoclonal antibodies, either Thy1.2-PE with B220-FITC (left) or CD4-PE with CD8-FITC (right) and FACS. (H) The tumor cells of the $CD3^+B220^-$ population did not express Vβ6.1 TCR (left), but showed weak expression of Vβ8.1-8.2 TCR (right). (I) Tumor cells from the liver (left) or spleen (right) were analyzed by staining with a combination of monoclonal antibodies, CD4-PE and CD8-FITC.

(FACS) analysis of the tumor cells showed that most of the lymphoma cells in the ascitic fluid and those that had invaded various organs were $CD4^+$ SP T cells (Figure 4F-H).

In the thymic tumor group, 16% of the homozygous mutant mice had large thymic tumors with a diameter of 1 to 3 cm (Figure 5A). Histologic analysis of the thymic tumors revealed that lymphoblastic lymphoma cells had densely proliferated in the cortex and medulla of the thymus (Figure 5B). Thymic lymphoma cells continuously invaded the lungs, chest wall, and pericardium (Figure 5C,D). In the peripheral lymph nodes, there was diffuse proliferation of monomorphic lymphoma cells focally mixed with tingible body macrophages, giving a "starry-sky" appearance (Figure 5E,F). In the thymic tumor group, surface marker analysis of thymic lymphoma cells revealed $CD4^+CD8^+$ DP T lymphoma cells (Figure 5G), which were negative for Vβ6.1 TCR and weakly positive for Vβ8.1-8.2 TCR with a single peak (Figure 5H). In this mouse, the mononuclear cells that invaded the liver, as well as a majority of the cells that invaded the spleen, were DP T lymphoma cells (Figure 5I). Therefore, in the same mouse, both tumor cells derived from the thymus and those that had invaded the organs were revealed to be DP T lymphoma cells. Moreover, the remaining mice with large thymic tumors showed the same $CD4^+CD8^+$ DP T lymphoma cells. In total, 84% of the T-cell tumors in *TCF8* homologous mutant mice could be classified as $CD4^+$ SP T-cell lymphoma, and 16%, as $CD4^+CD8^+$ DP thymic T-cell lymphoma. $CD8^+$ SP T lymphomas were never observed. Thus, the histopathological and cellular findings revealed that $CD4^+$ T-cell lymphoma/leukemia developed in most *TCF8* mutant mice.

Down-regulation of TCF8 expression is associated with TGF-β1 resistance in ATLL cells

The TGF-β superfamily is known to inhibit the lineage commitment of double-positive (DP) cells toward $CD4^+$ T-cell differentiation.[34] Interestingly, the ATLL cells were found to be resistant to growth inhibition by TGF-β1, even with high levels of TGF-β1 expression,[35-37] suggesting that ATLL cells may have developed several mechanisms of resistance to escape the antiproliferative and inactivating signal mediated by TGF-β1, including Tax through activation of the JNK/c-Jun pathway[38,39] or MEL1S expression.[37] Since TCF8 is reported to synergize with Smad

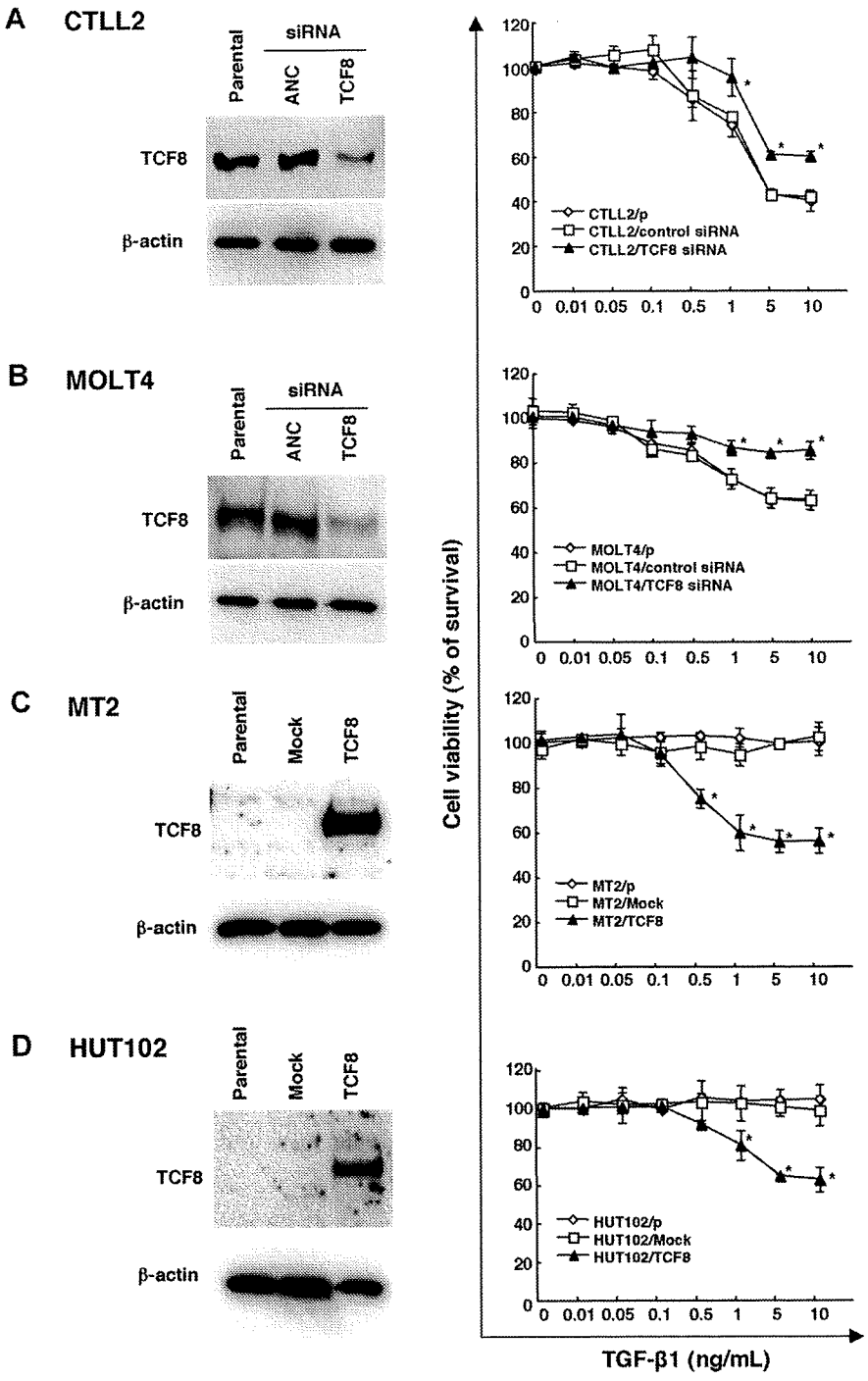

Figure 6. TGF-β1 responsiveness in various leukemia cell lines with the up- or down-regulation of TCF8 expression. (A,B) The down-regulation of the TCF8 protein by *TCF8* siRNA. The CTLL2 (A) and MOLT4 (B) cell lines were transfected with either *TCF8* or the AllStars Negative Control (ANC) siRNAs and then were incubated for 24 hours. The levels of TCF8 protein were examined in each cell line by Western blotting (left panel). After transfection with siRNAs, the cells were treated with the indicated concentrations of TGF-β1 for 72 hours. The degree of proliferation of each cell line was examined by MTT assay. The results are shown as percentages of the values obtained from the control TGF-β1–free culture (right panel). A ◇ represents parental cells, □ represents cells treated with ANC siRNA, and ▲ represents cells treated with *TCF8* siRNA. Student *t* test ($P < .05$) was used for the statistical analysis. (C,D) The enforced expression of TCF8 in HTLV-1–infected cell lines. The TCF8 protein levels were examined in each MT-2 (C) and HUT102 (D) cell transfected with a mock or TCF8 expression plasmid after 24 hours by Western blotting (left panel). The cells were treated with the indicated concentrations of TGF-β1 for 72 hours and the proliferation of each was examined by MTT assay. The results are shown as percentages of the values obtained from the control TGF-β1–free culture (right panel). Parental cells (◇), mock vector-transfected cells (□), and TCF8 expression plasmid-transfected cells (▲). All data are the means plus or minus standard deviation in a duplicate assay. Student *t* test ($P < .05$) was used for the statistical analysis.

proteins to activate TGF-β1 signal transduction,[40,41] we investigated whether the down-regulation of TCF8 expression was associated with resistance to TGF-β1–mediated growth inhibition in ATLL cells. Thereafter, either *TCF8* or ANC siRNA was introduced into a murine IL2–dependent T-lymphoma cell line, CTLL2, and human T-ALL cell line, MOLT4. Western blot analyses revealed the TCF8 expression in the siRNA-treated cells to be less than half of that in the control cells, while the viable cell curves of both cell lines treated with *TCF8* siRNA exhibited a significantly higher resistance to TGF-β1 than those of the control cells (Figure 6A,B). Next, the TCF8 expression plasmid was transiently introduced into 2 HTLV-1–infected T-cell lines (MT2 and HUT102) and up to 40% of the TCF8 transfectants died after TGF-β1 treatment in a dose-dependent manner, whereas the parental and transfectants with mock plasmid did not die with TGF-β1 treatment at all (Figure 6C,D). These results indicate that down-regulation of TCF8 expression is one of the mechanisms of TGF-β1 resistance in ATLL cells, suggesting that $CD4^+$ T lymphoma cells might escape from negative selection due to reduced TGF-β1 responsiveness.

Discussion

We demonstrated that in ATLL cells, the *TCF8* gene was mainly epigenetically inactivated in a majority of ATLL cells. In addition,

TCF8 (or $\delta EF1^{\Delta C\text{-}fin}$ homozygous) mutant mice frequently developed $CD4^+$ T-cell lymphoma and/or leukemia after a few months. These findings indicate that *TCF8* has a tumor suppressor role in ATLL. Since the heterozygous *TCF8* mutant mice did not develop any tumors and the level of TCF8 expression in some ATLL cells was approximately 30% to 40% of that observed in the control CD4 lymphocytes, TCF8 may therefore be involved in only some and not all of ATLL development. On the other hand, it is reported that *TCF8* overexpressed in colorectal or breast cancer cells induces epithelial-mesenchymal transition (EMT) with the development of metastatic properties such as migration and invasion in vitro and in vivo.[42] Therefore, *TCF8* has dual functions in cancer progression, which are dependent on the type of the tumors, such as *WT1* or *TSLC1* tumor suppressor genes.[43,44]

It was previously reported that *TCF8* mutant mice had a defect in T-cell development in the first week of life.[28] At the early stage of development, intrathymic c-kit$^+$ T precursor cells in these mice were depleted to just 1% of the level in normal mice, and the number of $CD8^+$ SP T cells was significantly reduced relative to the number of $CD4^+$ SP T cells. These observations indicate that TCF8 is involved in the regulation of T-cell development at multiple stages. Lymphoma cells in *TCF8* mutant mice showed either $CD4^+$ SP T cells or DP T cells after 6 months. Interestingly, TGF-β1 was important for regulating T-cell development in the thymus and for negative selection at the late stage of differentiation of DP T cells to $CD4^+$ SP cells.[34] Recently, DNA microarray analysis identified a higher level of *TCF8* expression in DP thymocytes to $CD4^+$ SP T cells,[45] suggesting that TCF8 enhanced negative selection due to TGF-β1 responsiveness. Moreover, *TGF-β1*–deficient mice had an increased number of $CD4^+$ SP T cells and a decreased number of $CD8^+$ SP T cells.[46,47] By correlating the development of $CD4^+$ SP T-lymphoma cells in *TCF8* mutant mice with the increase in the number of $CD4^+$ T cells in *TGF-β1*–deficient mice, we concluded that leukemogenesis in *TCF8* mutant mice was partly dependent on resistance to TGF-β1.

TCF8 is an E-box–binding transcription factor reported to regulate many genes. We found that the transcription of *CD4*, *α4 integrin*, and *GATA-3*, which was reported to be suppressed by TCF8,[48] was up-regulated in ATLL cells (data not shown). It was therefore suggested that impaired regulation of TCF8 expression in ATLL induced the increase in expression of *CD4* and *GATA3*, which was crucial for the establishment of the ATLL phenotype in $CD4^+$ SP helper T lymphocytes. Moreover, TCF8 was reported to regulate p73, CCNG2, or p130.[49,50] Since these genes are very important for cell-cycle progression and apoptosis, further investigation is needed to determine which ones are directly related to leukemogenesis among those regulated by TCF8.

The phenotypes of T-cell lymphomas in *TCF8* mutant mice were very similar to those of ATLL patients. In *TCF8* mutant mice, the tumor cells were mainly $CD4^+$ SP or DP T cells, which invaded various organs, such as the liver, spleen, and lungs. In ATLL, the tumor cells were mainly $CD4^+$ SP T cells that also invaded various organs. One difference, however, was that thymic lymphomas developed in the *TCF8* mutant mice, which has not been reported in ATLL cases. Another difference is that lymphoma cells in *TCF8* mutant mice did not have multilobulated nuclei. Such nuclei result from alterations in the PI3-kinase signaling cascades,[51] suggesting that down-regulation of TCF8 expression is not related to the PTEN signaling pathway and that other mutations are necessary for the development of ATLL. This is the first report illustrating the importance of the disruption of *TCF8* in leukemogenesis of ATLL.

Acknowledgments

We thank Drs M. Shiraga, I. Nishikata, and T. Uetsuki for technical assistance and advice on the paper.

This work was supported by Grants-in-Aid for Scientific Research of Priority Area and for 21st Century COE program (Life science) from the Ministry of Education, Culture, Sports, Science and Technology, Japan Leukemia Research fund, and Research fund from Miyazaki Prefecture Collaboration of Regional Entities for the Advancement of Technological Excellence, Japan Science and Technology Corporation.

Authorship

Contribution: T.H., S.N., and K.H. designed and performed experiments, analyzed data, and drafted the paper; M.H. performed experiments; T.K., Y.A., T.T., K.N., and M.T. performed experiments and data analysis; Y.A. and R.Y. performed the histopathology; K.Y., A.O., and H.T. collected case material and supervised the project; J.Y. and Y.H. supervised the project and drafted the paper; K.M. designed the experiments, analyzed data, and drafted the paper.

Conflict-of-interest disclosure: The authors declare no competing financial interests.

Correspondence: Kazuhiro Morishita, Division of Tumor and Cellular Biochemistry, Department of Medical Sciences, Faculty of Medicine, University of Miyazaki, 5200 Kihara, Kiyotake, Miyazaki, Japan, 889-1692; e-mail: kmorishi@med.miyazaki-u.ac.jp.

References

1. Takatsuki K, Yamaguchi K, Kawano F, et al. Clinical diversity in adult T-cell leukemia-lymphoma. Cancer Res. 1985;45:4644s-4645s.
2. Matsuoka M. Human T-cell leukemia virus type I and adult T-cell leukemia. Oncogene. 2003;22: 5131-5140.
3. Yoshida M. Multiple viral strategies of HTLV-1 for dysregulation of cell growth control. Annu Rev Immunol. 2001;19:475-496.
4. Tamiya S, Matsuoka M, Etoh K. Two types of defective human T-lymphotropic virus type I provirus in adult T-cell leukemia. Blood. 1996;88:3065-3073.
5. Koiwa T, Hamano-Usami A, Ishida T. 5′-long terminal repeat-selective CpG methylation of latent human T-cell leukemia virus type 1 provirus in vitro and in vivo. J Virol. 2002;76:9389-9397.
6. Okamoto T, Ohno Y, Tsugane S, et al. Multi-step carcinogenesis model for adult T-cell leukemia. Jpn J Cancer Res. 1989;80:191-195.
7. Look AT. Oncogenic transcription factors in the human acute leukemias. Science. 1997;278: 1059-1064.
8. Kamada N, Sakurai M, Miyamoto K, et al. Chromosome abnormalities in adult T-cell leukemia/lymphoma: a karyotype review committee report. Cancer Res. 1992;52:1481-1493.
9. Tsukasaki K, Krebs J, Nagai K, et al. Comparative genomic hybridization analysis in adult T-cell leukemia/lymphoma: correlation with clinical course. Blood. 2001;97:3875-3881.
10. Oshiro A, Tagawa H, Ohshima K, et al. Identification of subtype-specific genomic alterations in aggressive adult T-cell leukemia/lymphoma. Blood. 2006;107:4500-4507.
11. National Center for Biotechnology Information. GenBank. http://www.ncbi.nlm.nih.gov/site/entrez. Accessed December 12, 2007.
12. Williams TM, Moolten D, Burlein J, et al. Identification of a zinc finger protein that inhibits IL-2 gene expression. Science. 1991;25:1791-1794.
13. Barrallo-Gimeno A, Nieto MA. The Snail genes as inducers of cell movement and survival: implications in development and cancer. Development. 2005;132:3151-3161.
14. Thiery JP, Sleeman JP. Complex networks orchestrate epithelial-mesenchymal transitions. Nat Rev Mol Cell Biol. 2006;7:131-142.
15. Sasaki H, Nishikata I, Shiraga T, et al. Overexpression of a cell adhesion molecule, TSLC1, as

a possible molecular marker for acute-type adult T-cell leukemia. Blood. 2005;105:1204-1213.

16. Shimoyama M. Diagnostic criteria and classification of clinical subtypes of adult T-cell leukeamia-lymphoma: a report from the Lymphoma Study Group (1984-87). Br J Haematol. 1991;79:428-437.
17. Schneider U, Schwenk HU, Bornkamm G. Characterization of EBV-genome negative "null" and "T" cell lines derived from children with acute lymphoblastic leukemia and leukemic transformed non-Hodgkin lymphoma. Int J Cancer. 1977;19:621-626.
18. Minowada J, Onuma T, Moore GE. Rosette-forming human lymphoid cell lines. I. Establishment and evidence for origin of thymus-derived lymphocytes. J Natl Cancer Inst. 1972;49:891-895.
19. Yamada Y, Ohmoto Y, Hata T, et al. Features of the cytokines secreted by adult T cell leukemia (ATL) cells. Leuk Lymphoma. 1996;21:443-447.
20. Okada M, Maeda M, Tagaya Y, et al. TCGF (IL 2)-receptor induction Factor (S), II: possible role of ATL-derived factor (ADF) on constitutive IL 2 receptor expression of HTLV-1(+) T cell lines. J Immunol. 1985;135:3995-4003.
21. Miyoshi I, Kubonishi I, Yoshimoto S, et al. Type C virus particles in a cord T-cell line derived by cocultivating normal human cord leukocytes and human leukaemic T cells. Nature. 1981;294:770-771.
22. Gillis S, Smith KA. Long term culture of tumour-specific cytotoxic T cells. Nature. 1977;268:154-156.
23. Shaffer LG, Tommerup N (eds). ISCN (2005): An International System for Human Cytogenetic Nomenclature. S. Karger, Basel; 2005.
24. Kakazu N, Taniwaki M, Horiike S, et al. Combined spectral karyotyping and DAPI banding analysis of chromosome abnormalities in myelodysplastic syndrome. Gene Chromosome Cancer. 1999;26:336-345.
25. Taniwaki M, Nishida K, Ueda Y, et al. Interphase and metaphase detection of the breakpoint of 14q32 translocations in B-cell malignancies by double-color fluorescence in situ hybridization. Blood. 1995;85:3223-3228.
26. National Center for Biotechnology Information. http://www.ncbi.nlm.nih.gov/project/genome. Accessed December 12, 2007.
27. Nannya Y, Sanada M, Nakazaki K, et al. A robust algorithm for copy number detection using high-density oligonucleotide single nucleotide polymorphism genotyping arrays. Cancer Res. 2005;65:6071-6079.
28. Higashi Y, Moribe H, Takagi T, et al. Impairment of T cell development in deltaEF1 mutant mice. J Exp Med. 1997;185:1467-1479.
29. Takagi T, Moribe H, Kondoh H, Higashi Y. DeltaEF1, a zinc finger and homeodomain transcription factor, is required for skeleton patterning in multiple lineages. Development. 1998;125:21-31.
30. Hark AT, Schoenherr CJ, Katz DJ, et al. CTCF mediates methylation-sensitive enhancer-blocking activity at the H19/Igf2 locus. Nature. 2000;405:486-489.
31. Bell AC, Felsenfeld G. Methylation of a CTCF-dependent boundary controls imprinted expression of the Igf2 gene. Nature. 2000;405:482-485.
32. Schmelz K, Wagner M, Dörken B, Tamm I. 5-Aza-2'-deoxycytidine induces p21WAF expression by demethylation of p73 leading to p53-independent apoptosis in myeloid leukemia. Int J Cancer. 2005;114:683-695.
33. Soengas MS, Capodieci P, Polsky D. Inactivation of the apoptosis effector Apaf-1 in malignant melanoma. Nature. 2001;409:207-211.
34. Licona-Limon P, Soldevila G. The role of TGF-beta superfamily during T cell development: new insights. Immunol Lett. 2007;109:1-12.
35. Niitsu Y, Urushizaki Y, Koshida Y, et al. Expression of TGF-beta gene in adult T cell leukemia. Blood. 1988;71:263-266.
36. Kim SJ, Kehrl JH, Burton J, et al. Transactivation of the transforming growth factor beta 1 (TGF-beta 1) gene by human T lymphotropic virus type 1 tax: a potential mechanism for the increased production of TGF-beta 1 in adult T cell leukemia. J Exp Med. 1990;172:121-129.
37. Yoshida M, Nosaka K, Yasunaga J, Nishikata I, Morishita K, Matsuoka M. Aberrant expression of the MEL1S gene identified in association with hypomethylation in adult T-cell leukemia cells. Blood. 2004;103:2753-2760.
38. Arnulf B, Villemain A, Nicot C, et al. Human T-cell lymphotropic virus oncoprotein Tax represses TGF-beta 1 signaling in human T cells via c-Jun activation: a potential mechanism of HTLV-I leukemogenesis. Blood. 2002;100:4129-4138.
39. Xu X, Heidenreich O, Kitajima I, et al. Constitutively activated JNK is associated with HTLV-1 mediated tumorigenesis. Oncogene. 1996;13:135-142.
40. Postigo AA. Opposing functions of ZEB proteins in the regulation of the TGFβ/BMP signaling pathway. EMBO J. 2003;22:2443-2452.
41. Postigo AA, Depp JL, Taylor JJ, Kroll KL. Regulation of Smad signaling through a differential recruitment of coactivators and corepressors by ZEB proteins. EMBO J. 2003;22:2453-2462.
42. Peinado H, Olmeda D, Cano A. Snail, Zeb and bHLH factors in tumour progression: an alliance against the epithelial phenotype? Nat Rev Cancer. 2007;7:415-428.
43. Murakami Y. Involvement of a cell adhesion molecule, TSLC1/IGSF4, in human oncogenesis. Cancer Sci. 2005;96:543-552.
44. Yang L, Han Y, Saurez Saiz F, Minden MD. A tumor suppressor and oncogene: the WT1 story. Leukemia. 2007;21:868-876.
45. Dik WA, Pike-Overzet K, Weerkamp F, et al. New insights on human T cell develoment by quantitative T cell receptor gene rearrangement studies and gene expression profiling. J Exp Med. 2005;201:1715-1723.
46. Christ M, McCartney-Francis NL, Kulkarni AB, et al. Immune dysregulation in TGF-β1-deficient mice. J Immunol. 1994;153:1936-1946.
47. Plum J, De Smedt M, Leclercq G, Vandekerckhove B. Influence of TGF-β on murine thymocyte development in fetal thymus organ culture. J Immunol. 1995;154:5789-5798.
48. Postigo AA, Dean DC. Independent repressor domains in ZEB regulate muscle and T-cell differentiation. Mol Cell Biol. 1999;19:7961-7971.
49. Fontemaggi G, Gurtner A, Damalas A, et al. δEF1 repressor controls selectively p53 family members during differentiation. Oncogene. 2005;24:7273-7280.
50. Chen J, Yusuf I, Andersen HM, Fruman DA. FOXO transcription factors cooperate with δEF1 to activate growth suppressive genes in B lymphocytes. J Immunol. 2006;176:2711-2721.
51. Fukuda R, Hayashi A, Utsunomiya A, et al. Alteration of phosphatidylinositol 3-kinase cascade in the multilobulated nuclear formation of adult T cell leukemia/lymphoma (ATLL). Proc Natl Acad Sci U S A. 2005;102:15213-15218.

Novel gain-of-function mutation in the extracellular domain of the *PDGFRA* gene in infant acute lymphoblastic leukemia with t(4;11)(q21;q23)

Leukemia (2008) **22,** 2279–2280; doi:10.1038/leu.2008.140; published online 12 June 2008

Platelet-derived growth factor receptors α and β (PDGFRA and PDGFRB) belong to the class III receptor tyrosine kinases, which include c-KIT, colony stimulating factor-1 receptor and FLT3.[1] *PDGFRA* and *c-KIT* are two related receptor tyrosine kinases showing similar structure, and mutations of these genes are detected in gastrointestinal stromal tumor[2,3] and myeloproliferative disorders.[4] Recently, we reported a *PDGFRA* N870S mutation in a 13-year-old boy having acute myelogenous leukemia (AML)-M1 with t(8;21) and an F808L mutation in a 13-year-old girl having AML-M1 with inv(16).[5] In addition to point mutations, the *FIP1L1-PDGFRA* fusion tyrosine kinase resulting from internal deletion of 4q12 locus was described in a subgroup of patients presenting hypereosinophilic syndrome.[6] Here, we investigated whether *PDGFRA* is also implicated in the pathogenesis of acute lymphoblastic leukemia (ALL), and found a mutation which renders a factor-dependent cell line factor-independent by its aberrant tyrosine phosphorylation.

One hundred and twenty seven childhood ALL and 40 infant ALL samples, including those from 13 patients with t(4;11)(q21;q23) (one patient was childhood ALL and the others were infant ALL), were analyzed for the expression and mutation of *PDGFRA*. *PDGFRA* gene was expressed in 38 (29.9%) of the 127 childhood ALL patient samples, 12 (30.0%) of the 40 infant ALL patients and 9 (36.0%) of the 25 ALL patients associated with *MLL* gene rearrangements. Sequence analyses of the samples expressing *PDGFRA* revealed a *PDGFRA* A509D mutation (Figure 1a) in a 4-month-old boy having ALL with t(4;11)(q21;q23). This mutation in the Ig5 domain of *PDGFRA* corresponds to those responsible for ligand-independent kinase activation of *c-KIT* in gastrointestinal stromal tumor.[3] Mutations on exon 9 encoding the extracellular domain near the transmembrane domain of *c-KIT* lead to ligand-independent activation of c-KIT,[2,3] and are associated with core binding factor AML and gastrointestinal stromal tumor.[1,3,7] We examined whether the mutation at Ig5 domain of the *PDGFRA* gene resulted in constitutive activation of the kinase activity by retroviral transduction[8] of the wild-type and mutated *PDGFRA* cDNAs into an IL-3 dependent mouse cell line, Ba/F3 and stable cell lines expressing each transgene were established. The whole coding region of *PDGFRA* cDNA was sequenced directly or after subcloning into a retroviral vector pMXs-IN(IRES-Neo).[8] The empty vector as a negative control was also introduced into Ba/F3 cells. As expected, the wild-type PDGFRA was not significantly phosphorylated on tyrosine residues in the absence of PDGF (Figure 1b). In contrast, the PDGFRA with the Ig5 domain A509D mutation was phosphorylated in the absence of PDGF (Figure 1b). Because the signal transduction pathway of PDGFRA is comparable with that of c-KIT,[2] the gain-of-function mutations of PDGFRA by themselves may transform Ba/F3 cells. In fact, Ba/F3 cells expressing the A509D mutant PDGFRA grew in the absence of IL-3 and PDGF whereas those expressing the wild-type did not (data not shown). It is possible that the mutant PDGFRA may contribute to leukemogenesis with t(4;11).

In conclusion, we reported the frequency of *PDGFRA* mutations in a large series of Japanese pediatric and infantile ALL patients. This is the first report showing a constitutively active *PDGFRA* mutation found in an ALL patient that may be associated with leukemic cell growth.

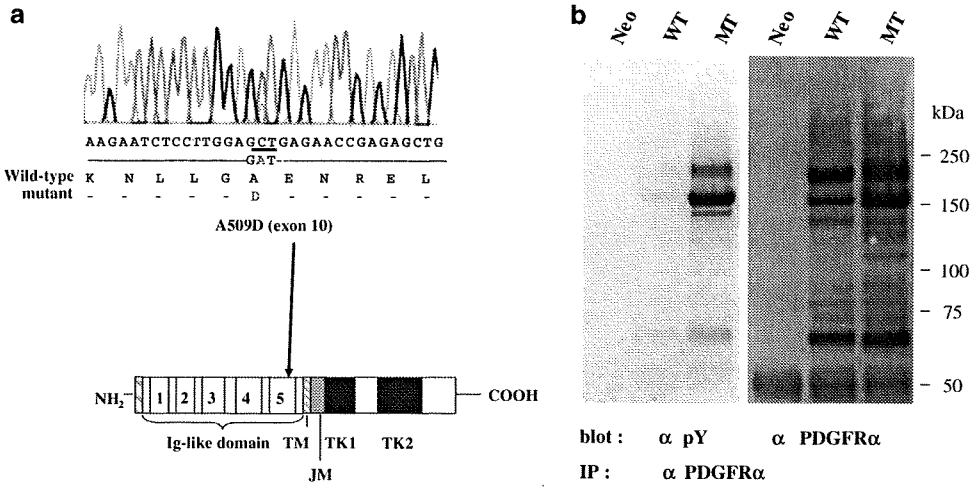

Figure 1 cDNA sequencing and position of the mutation of the *platelet-derived growth factor receptor α* (*PDGFRA*) gene at the Ig5 domain and tyrosine phosphorylation of the PDGFRA mutant. (**a**) Direct sequencing of the PCR product for the *PDGFRA* from an ALL patient with t(4;11) demonstrates the wild-type (WT) (top), and the A509D mutant (bottom) alleles. (**b**) Functional analysis of the WT PDGFRA and the A509D mutant derived from an ALL with t(4:11) patient. The mutant (MT), but not the WT PDGFRA was phosphorylated on tyrosine residues in Ba/F3 cells after retroviral transduction. Ba/F3 cells transduced with the empty vector (Neo) and those with the WT expressor were cultured with IL-3, and those with the MT expressor were cultured without IL-3. Lysates were prepared from cultured cells, immunoprecipitated with a polyclonal antibody to PDGFRA (sc-338, Santa Cruz Biotechnology, Santa Cruz, CA, USA), and immunoblotted with an anti-phosphotyrosine (pY) monoclonal antibody (Upstate Biotechnology, Inc., Lake Placid, NY, USA) (left panel), and with the anti-PDGFRA antibody (sc-338) (right panel). There was no detectable phosphorylation of WT PDGFRA. IP, immunoprecipitation. Ig, immunoglobulin; TM, transmembrane domain; JM, juxtamembrane domain; TK1 and TK2, two intracellular kinase domains.

Acknowledgements

We thank S Sohma and H Soga for technical assistance. We also thank Dr S Hirota for wild-type PDGFRA expression plasmid. This work was supported by a Grant-in-Aid for Cancer Research from the Ministry of Health, Labor, and Welfare of Japan, a Grant-in-Aid for Scientific Research on Priority Areas, and Grants-in-Aid from the Ministry of Education, Culture, Sports, Science and Technology of Japan.

M Hiwatari[1,4], R Ono[2,4], T Taki[3], A Hishiya[4], E Ishii[5], T Kitamura[4], Y Hayashi[6] and T Nosaka[2,4]
[1]*Department of Pediatrics, Graduate School of Medicine, The University of Tokyo, Tokyo, Japan;*
[2]*Department of Microbiology, Mie University Graduate School of Medicine, Tsu, Japan;*
[3]*Department of Molecular Laboratory Medicine, Kyoto Prefectural University of Medicine Graduate School of Medical Science, Kyoto, Japan;*
[4]*Division of Cellular Therapy, The Institute of Medical Science, The University of Tokyo, Tokyo, Japan;*
[5]*Department of Pediatrics, Ehime University Graduate School of Medicine, Ehime, Japan and*
[6]*Gunma Children's Medical Center, Gunma, Japan*
E-mail: nosaka@doc.medic.mie-u.ac.jp or hayashiy-tky@umin.ac.jp

References

1 Blume-Jensen P, Hunter T. Oncogenic kinase signalling. *Nature* 2001; **411**: 355–365.
2 Fletcher JA. Role of KIT and Platelet-Derived Growth Factor Receptors as Oncoproteins. *Seminars in Oncology* 2004; **31**: 4–11.
3 Hirota S, Nishida T, Isozaki K, Taniguchi M, Nakamura J, Okazaki T *et al.* Gain-of-function mutation at the extracellular domain of KIT in gastrointestinal stromal tumours. *Journal of Pathology* 2001; **193**: 505–510.
4 Tefferi1 A, Gilliland DG. Oncogenes in Myeloproliferative Disorders. *Cell Cycle* 2007; **5**: 550–566.
5 Hiwatari M, Taki T, Tsuchida M, Hanada R, Hongo T, Sako M *et al.* Novel missense mutations in the tyrosine kinase domain of the platelet-derived growth factor receptor alpha(PDGFRA) gene in childhood acute myeloid leukemia with t(8;21)(q22;q22) or inv(16)(p13q22). *Leukemia* 2005; **19**: 476–477.
6 Burgstaller S, Kreil S, Waghorn K, Metzgeroth G, Preudhomme C, Zoi K *et al.* The severity of *FIP1L1–PDGFRA*-positive chronic eosinophilic leukaemia is associated with polymorphic variation at the *IL5RA* locus. *Leukemia* 2007; **21**: 2428–2432.
7 Wang YY, Zhou GB, Yin T, Chen B, Shi JY, Liang WX *et al. AML1–ETO* and *C-KIT* mutation/overexpression in t(8;21) leukemia: Implication in stepwise leukemogenesis and response to Gleevec. *Proc Natl Acad Sci USA* 2005; **102**: 1104–1109.
8 Kitamura T, Koshino Y, Shibata F, Oki T, Nakajima H, Nosaka T *et al.* Retrovirus-mediated gene transfer and expression cloning: Powerful tools in functional genomics. *Exp Hematol* 2003; **31**: 1007–1014.

Clinical and biological significance of *RAS* mutations in multiple myeloma

Leukemia (2008) **22**, 2280–2284; doi:10.1038/leu.2008.142; published online 5 June 2008

Primary genetic abnormalities in myeloma (MM) such as trisomies of chromosomes 3, 5, 7, 9, 11, 15, 19 and 21 associated with hyperdiploid MM and translocations involving the immunoglobulin heavy chain (IgH) locus on chromosome 14q32 and three main recurrent partners: MMSET/FGFR3, CCND1 and c-MAF are already present in the pre-malignant monoclonal gammopathy of undetermined significance (MGUS) stage.[1] Some patients with these genetic abnormalities may remain as MGUS for many years without transforming to MM, suggesting that they are involved in clonal initiation but do not mediate malignant transformation.

One of the recurrent differences between MGUS and MM is the presence of *RAS* mutations in the latter. *RAS* mutations may, therefore, play an important role in malignant transformation of clonal plasma cells and myeloma pathogenesis. However, the clinical and biological significance of *RAS* mutation in MM has not been clearly established as most of the previous studies have involved small numbers of heterogeneously treated patients.

To establish the clinical and biological significance of *RAS* mutation in MM, we studied the association of *RAS* mutation with a comprehensive spectrum of clinical parameters including the newly established ISS staging and survival, as well as a panel of known recurrent genetic abnormalities in MM such as t(4;14), t(14;16), t(11;14), chromosome 13 and 17p13 deletion detected by fluorescent *in situ* hybridization[2] and ploidy assessed by DNA content measurement using flow cytometry,[3] in a large cohort of newly diagnosed patients enrolled in the Eastern Cooperative Group (ECOG) clinical trial E9486/E9487 ($N=561$).[4] A total of 439 patients, based on sample availability, were included (The ECOG Cohort). For this cohort, DNA from unsorted whole bone marrow was used for *RAS* mutation studies. We also studied 14 MGUS patients and 82 MM patients (60 newly diagnosed and 22 relapsed) from the Mayo Clinic (Mayo Cohort). Bone marrow samples were obtained after informed consent according to the Declaration of Helsinki. The study was approved by the Mayo Clinic Institution Review Board. CD138 positive plasma cells were enriched using immuno-magnetic beads (AutoMACS; Miltenyi-Biotec, Auburn, CA, USA). RNA and DNA from these enriched cells were used for gene expression and *RAS* mutation studies, respectively.

Conformation sensitive gel electrophoresis was used to screen samples for *KRAS* (codons 12, 13 and 61) and *NRAS* (codons 12, 13 and 61) mutations (Supplementary Methods). *RAS* mutation was detected in 102 (23%) patients in the ECOG cohort. Seventy-four (17%) patients had mutations in *NRAS*. The majority of these mutations were in codon 61 (64 of the 74), with 5 mutations detected in codons 12 and 13. We also found mutations in codon 64 ($n=1$) and codon 86 ($n=4$). Twenty-eight (6%) patients had mutations in K-*RAS*. Twenty-two of these are in codons 12 and 13 and three in codon 61. In addition, we also found one mutation each in codon 16, 22 and 24. In the Mayo Clinic cohort, *RAS* mutation was detected in 1 of 14 MGUS patients (7%), 15 of 60 newly diagnosed MM patients (25%) and 10 of 22 relapsed MM patients (45%). Once again N-*RAS* mutations were more common that K-*RAS* mutations. Our study confirms the low incidence of *RAS* mutation in MGUS compared to MM found in a previous study,[5] consistent with

A Novel FLT3 Inhibitor FI-700 Selectively Suppresses the Growth of Leukemia Cells with FLT3 Mutations

Hitoshi Kiyoi,[1] Yukimasa Shiotsu,[2] Kazutaka Ozeki,[1] Satomi Yamaji,[1] Hiroshi Kosugi,[3] Hiroshi Umehara,[2] Makiko Shimizu,[2] Hitoshi Arai,[2] Kenichi Ishii,[2] Shiro Akinaga,[2] and Tomoki Naoe[4]

Abstract **Purpose:** The aim of this study was to evaluate the antileukemia activity of a novel FLT3 kinase inhibitor, FI-700.

Experimental Design: The antileukemia activity of FI-700 was evaluated in human leukemia cell lines, mutant or wild-type (Wt)-FLT3–expressing mouse myeloid precursor cell line, 32D and primary acute myeloid leukemia cells, and in xenograft or syngeneic mouse leukemia models.

Results: FI-700 showed a potent IC_{50} value against FLT3 kinase at 20 nmol/L in an *in vitro* kinase assay. FI-700 showed selective growth inhibition against mutant FLT3-expressing leukemia cell lines and primary acute myeloid leukemia cells, whereas it did not affect the FLT3 ligand (FL)–driven growth of Wt-FLT3–expressing cells. These antileukemia activities were induced by the significant dephosphorylations of mutant FLT3 and STAT5, which resulted in G_1 arrest of the cell cycle. Oral administration of FI-700 induced the regression of tumors in a s.c. tumor xenograft model and increased the survival of mice in an i.v. transplanted model. Furthermore, FI-700 treatment eradicated FLT3/ITD-expressing leukemia cells, both in the peripheral blood and in the bone marrow. In this experiment, the depletion of FLT3/ITD-expressing cells by FI-700 was more significant than that of Ara-C, whereas bone marrow suppression by FI-700 was lower than that by Ara-C.

Conclusions: FI-700 is a novel and potent FLT3 inhibitor with promising antileukemia activity.

FLT3 (FMS-like receptor tyrosine kinase) also referred to as fetal liver kinase 2 or stem cell tyrosine kinase 1 is a class III receptor tyrosine kinase together with KIT, FMS, and platelet-derived growth factor receptor (1, 2). Class III receptor tyrosine kinases share several structural characteristics including five immunoglobulin-like domains in the extracellular region, a juxtamembrane domain, a tyrosine kinase domain separated by a kinase insert domain, and a COOH-terminal domain in the intracellular region (3). Several mutations of receptor tyrosine kinases, found in human and murine malignancies, have been implicated in the constitutive activation of kinases (4). In 1996, a unique mutation of the *FLT3* gene was first identified in acute myeloid leukemia (AML) cells (5). This mutation (FLT3/ITD) is formed when a fragment of the juxtamembrane domain–coding sequence is duplicated in a direct head-to-tail orientation (6). Subsequently, a missense point mutation at the D835 residue and point mutations, deletions, and insertions in the codons surrounding D835 within a tyrosine kinase domain of FLT3 (FLT3/KDM) have been found (7). To date, a number of studies, involving >5,000 individuals, have shown that FLT3/ITD and FLT3/KDM occur in 15% to 35% and 5% to 10% of adults with AML, respectively (8). Mutations of the *FLT3* gene are, therefore, the most frequent genetic alterations thus far reported as involved in AML. Several large-scale studies in well-documented patients published to date have shown the effect on the clinical outcome in patients with *FLT3* mutations (8). Interestingly, FLT3/ITD is far less common in patients with ALL, whereas FLT3/KDM is recurrently found in patients with ALL, especially in those harboring an *MLL* gene rearrangement or hyperdiploidy (9–11). It is notable that FLT3 is highly expressed in *MLL* gene–rearranged ALL, leading to the constitutive activation of wild-type FLT3 kinase, and that primary ALL cells, which strongly express FLT3, but do not carry *FLT3* mutations, have the same sensitivity to a potent FLT3 inhibitor as leukemia cells with *FLT3* mutations (12). Recently, remarkably high levels of FLT3 transcripts have been shown in a proportion of AML patients without *FLT3* mutations, which are associated with a poor prognosis for overall survival (13). These results indicate that FLT3 is greatly involved in the pathophysiology both of AML and ALL. However, the optimal treatment strategy for patients with *FLT3* mutations should be further evaluated because it remains unclear whether high-dose chemotherapy and/or myeloablative therapy supported by hematopoietic stem cell transplantation

Authors' Affiliations: [1]Department of Infectious Diseases, Nagoya University School of Medicine, [2]Pharmaceutical Research Center of Kyowa Hakko Kogyo, Shizuoka, Japan; [3]Department of Hematology, Ogaki Municipal Hospital, Ogaki, Japan; and [4]Department of Hematology and Oncology, Nagoya University Graduate School of Medicine, Nagoya, Japan

Received 1/29/07; revised 4/19/07; accepted 5/9/07.

Grant support: National Institute of Biomedical Innovation (T. Naoe); Ministry of Health, Labor, and Welfare (T. Naoe); Ministry of Education, Culture, Sports, Science and Technology grant for Scientific Research (T. Naoe and H. Kiyoi); and the 21st Century COE Program "Integrated Molecular Medicine for Neuronal and Neoplastic Disorders" (T. Naoe), Japan.

The costs of publication of this article were defrayed in part by the payment of page charges. This article must therefore be hereby marked *advertisement* in accordance with 18 U.S.C. Section 1734 solely to indicate this fact.

Note: H. Kiyoi, Y. Shiotsu, and K. Ozeki contributed equally to this work.

Requests for reprints: Hitoshi Kiyoi, Department of Infectious Diseases, Nagoya University School of Medicine, 65 Tsurumai-cho, Showa-ku, Nagoya 466-8560, Japan. Phone: 81-52-744-2955; Fax: 81-52-744-2801; E-mail: kiyoi@med.nagoya-u.ac.jp.

doi:10.1158/1078-0432.CCR-07-0225

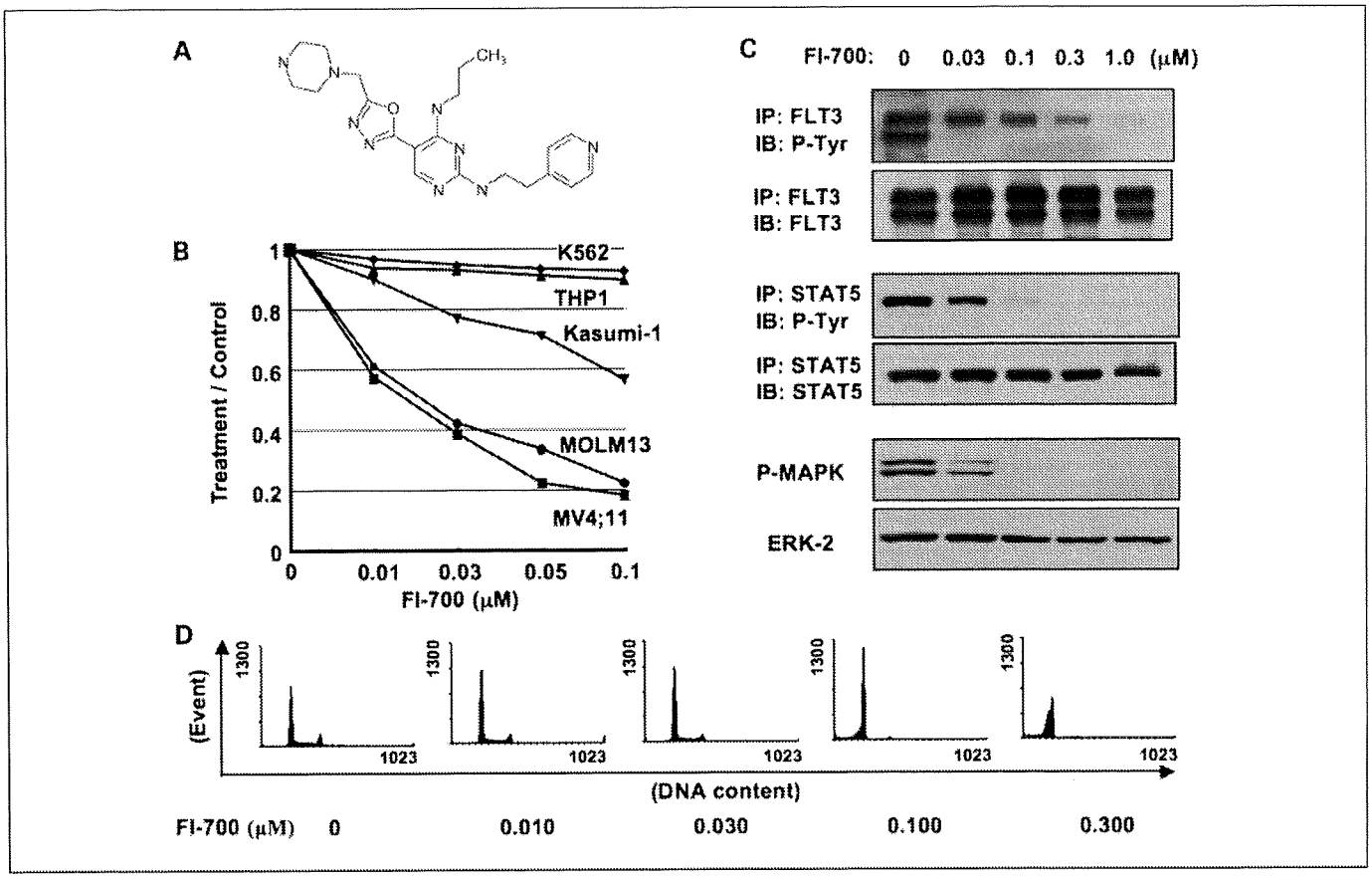

Fig. 1. Effects of FI-700 on cell growth and mutant FLT3-mediated signals. *A*, chemical structure of FI-700. *B*, growth inhibition effect on human leukemia cell lines was evaluated by measuring viable cells after treatment with FI-700 for 72 h. FI-700 selectively and sensitively inhibits the growth of FLT3/ITD-carrying leukemia cell lines MV4;11 and MOLM13 with IC_{50} values of 0.014 and 0.016 μmol/L, respectively. FI-700 is also potent against Kasumi-1, whereas its growth-inhibitory activity was ~10 times lower than that against MV4;11 or MOLM13. *C*, MOLM13 cells were treated with increasing concentrations of FI-700 for 6 h. Phosphorylation status of FLT3, STAT5, and MAPK were examined by Western blot analysis. FI-700 dose-dependently inhibits the constitutive phosphorylation of mutant FLT3 as well as its downstream molecules STAT5 and MAPK. *D*, MOLM13 cells were treated with increasing concentrations of FI-700 for 24 h. After treatment, the cells showed an increase in the percentage of G_1 cells and a reciprocal reduction in the percentage of the S phase. Apparent increase of sub-G_1 apoptotic cells was also observed at >0.10 μmol/L of FI-700.

could conquer the adverse effects of *FLT3* mutations (14). Therefore, mutated or overexpressed FLT3, which leads to constitutive active kinase, serves as an important molecular target in the treatment of leukemia (15, 16). To date, several inhibitors, such as PKC412, CEP-701, MLN-518, or SU-11248 have been subjected to clinical trials in several hematologic malignancies including AML (17–20). However, the clinical efficacy of these FLT3 inhibitors in patients with AML seems unimpressive, possibly because of the potency, adverse events, or protein binding of each drug (21, 22). In addition, most of these kinase inhibitors, which are currently in development, were not originally screened for sensitivity and selectivity against the activated FLT3 kinase. Therefore, the discovery and clinical development of second generation novel FLT3 inhibitors is required. In this study, we evaluated the effects of FI-700, a novel FLT3 kinase inhibitor, on leukemia cells both *in vitro* and *in vivo*.

Materials and Methods

Drugs. Drugs such as FI-700 and MLN-518 were synthesized at the Pharmaceutical Research Center of Kyowa Hakko Kogyo. Ara-C (cytarabine) was purchased from Sankyo Pharmaceuticals. Drugs were prepared as a 10 mmol/L DMSO solution and stored at -20°C until use and freshly diluted with cell culture medium.

Kinase assays for FI-700. To evaluate the kinase inhibitory activities of FI-700 against FLT3 in a cell-free system, a commercially available FLT3 enzyme (recombinant human COOH-terminal 564-end amino acids; Upstate Biotechnology) and its substrate biotinylated poly-(Glu/Tyr 4:1) substrate (CISbio International) were used. FI-700 inhibition of substrate phosphorylation by a series of tyrosine and serine/threonine kinases was analyzed as previously described (23).

Cell lines and cell culture. Human leukemia cell line, MOLM-13, was obtained from DSMZ (German Resource Centre for Biological Material); MV4;11, THP1, K562, and HL60 were from the American Type Culture Collection; Kasumi-1 was from Hiroshima University; whereas MegO1 was established at Nagoya University. MV4;11 was maintained in Iscove's modified Dulbecco's medium (Life Technologies) supplemented with 10% FCS, and the other human leukemia cell lines were in RPMI 1640 supplemented with 10% FCS. It was found that MOLM-13 and MV4;11 have FLT3/ITD, THP1 expresses wild-type (Wt)-FLT3 protein on their surfaces, K562 and MegO1 have a *BCR/ABL* translocation, Kasumi-1 has a *RUNX1/MTG8* translocation and a *c-KIT* mutation, and that HL60 does not express FLT3 protein. A murine IL-3–dependent myeloid progenitor cell line, 32D, was obtained from the RIKEN Cell Bank, and maintained in RPMI 1640 (Life Technologies) supplemented with 10% FCS (Life Technologies) and 1 ng/mL murine IL-3 (R&D Systems). Wt-FLT3-, FLT3/ITD-, and FLT3/D835Y–expressing 32D cells were previously reported (7, 24, 25). Wt-FLT3–expressing 32D cells were maintained in

RPMI 1640 supplemented with 10% FCS and 1 ng/mL of murine IL-3. FLT3/ITD- and FLT3/D835Y-expressing 32D cells were maintained in RPMI 1640 supplemented with 10% FCS without IL-3. Furthermore, we cloned human FLT3/ITD cDNA into the pMX-internal ribosomal entry site-green fluorescent protein (GFP) vector (kindly provided by Professor Toshio Kitamura, Tokyo University, Japan), transduced into 32D cells as previously described, and established stable FLT3/ITD-GFP-expressing 32D cells (FLT3/ITD-GFP-32D). FLT3/ITD-GFP-32D cells revealed autonomous proliferation at the same level as FLT3/ITD- and FLT3/D835Y-expressing 32D cells, and were maintained in RPMI 1640 supplemented with 10% FCS without IL-3.

Primary patient samples. Bone marrow (BM) samples from patients with AML were subjected to Ficoll-Hypaque (Pharmacia LKB) density gradient centrifugation. All samples were morphologically confirmed to contain >90% leukemia cells after centrifugation on May-Grünwald Giemsa-stained cytospin slides, and then cryopreserved in liquid nitrogen before use. Informed consent was obtained from all patients for the use of their samples for the present study, as well as banking and molecular analysis. Approval for this study was obtained from the ethical committees of Nagoya University and Ogaki Municipal Hospital. Each karyotype was determined by standard G-banding analysis. Mutations of the *FLT3* gene were examined as previously reported (7, 26, 27).

Growth inhibition and cell cycle analyses. Cell lines and primary AML cells were suspended in RPMI 1640 (Life Technologies) containing 10% FCS, and 2×10^4 cells per well were seeded in 96-well culture plates with or without FI-700. Cell viability was measured using the CellTiter^{96} Proliferation Assay (Promega) according to the instructions of the manufacturer. These procedures were done thrice independently.

For cell cycle analysis, MOLM-13 cells (3×10^4) were treated with increasing concentrations of FI-700 for 24 h. DNA contents were analyzed as previously described (28).

Western blot analysis. Anti-phospho-MAPK and anti-ERK2 antibodies were purchased from New England Biolabs. Anti-FLT3 and anti-STAT5A antibodies were from Santa Cruz Biotechnology. Anti-phosphotyrosine antibody 4G10 was from Upstate Biotechnology. Anti-phospho-STAT5 mouse monoclonal antibody was prepared in the Pharmaceutical Research Center of Kyowa Hakko Kogyo. Cell lysates were extracted, separated by SDS-PAGE, and electroblotted onto Immobilon PVDF membranes (Millipore), as previously described (24). FLT3 proteins were immunoprecipitated with anti-FLT3 antibodies. The precipitated samples were subjected to immunoblot analysis to detect the tyrosine phosphorylation using an antiphosphotyrosine antibody (4G10). The membranes were incubated with stripping buffer, and then reprobed with anti-FLT3 antibody.

In vivo ***antileukemia effects on xenograft transplantation.*** Severe combined immunodeficiency (SCID) mice (Fox Chase C.B-17/Icr-scidJcl, male, 5 weeks old) were purchased from CLEA Japan. Mice were treated with an i.p. injection of anti-asialo-GM1 antibody (0.3 mg/mouse; Wako Pure Chemical Industries). The day after anti-asialo-GM1 antibody treatment, all mice were s.c. inoculated in the shaved area with 1×10^7 of MOLM-13. Five days after inoculation, tumor volume was measured using the Antitumor test system II (Human Life), the computer operation system with the software program and instruments. Twenty-five mice with tumors ranging from 90 to 130 mm^3 were selected and randomized using the Antitumor test system II. The selected mice were divided into five groups (five mice each), and FI-700 (100 or 200 mg/kg b.i.d.) was given orally (p.o.) for 5 days from the 7th day after inoculation. Because our preliminary study showed that the administration of 400 mg/kg b.i.d. for 5 days induced body weight loss in SCID mice, we selected this treatment schedule (data not shown). The tumor volume was measured every 2 days for 10 days. Tumor volume was calculated by the Antitumor test system II as follows: tumor volume = $D_L \times D_S \times D_S \times 1/2$ (D_L, long diameter; D_S, short diameter). Relative tumor volume was represented as V/V_0 (V_0, initial tumor volume; V, tumor volume after dosing). The relative V/V_0 value on each day was represented as T/C (C, V/V_0 of vehicle-treated control mouse; T, V/V_0 of FI-700-treated mouse). We also compared the antileukemia effects between FI-700 and other potent FLT3 inhibitors, MLN-518 and PKC-412, in the same xenograft model. The MOLM-13 inoculated SCID mice were administered with MLN-518 (160 mg/kg b.i.d.) or PKC-412 (400 mg/kg q.d.) for 5 days. These doses of MLN-518 and PKC-412 were selected as the maximum tolerated dose according to previous reports (29, 30) and our preliminary examinations.

In the other xenograft model, SCID mice, treated with anti-asialo-GM1 antibody, were i.v. inoculated with 1×10^7 of MOLM-13 cells. Thirteen days after inoculation, mice were randomized and divided into three groups (five mice each). From the day after randomization, mice were given FI-700 at 200 mg/kg (p.o.) b.i.d., Ara-C at 75 mg/kg (i.v.) b.i.d., or vehicle for 3 days. In our preliminary study, the i.v. administration of Ara-C at 150 mg/kg q.d. for 5 days induced severe body weight loss and occasionally (not always) killed animals in leukemia-transplanted status, whereas that of Ara-C at 75 mg/kg b.i.d. for 5 days was tolerable. We, therefore, decided that 75 mg/kg/d was the maximum tolerated dose in our experiment model.

In vivo ***antileukemia effects on syngeneic transplantation.*** C3H/Hej mice were purchased from Charles River Japan. Fifteen mice were i.v. inoculated with 2×10^6 of FLT3/ITD-GFP-32D cells, then randomly divided into three groups (five mice each). On the 7th day after inoculation, peripheral blood (PB) was collected from the mice. From the 10th day after inoculation, mice were given FI-700 at 200 mg/kg (p.o.) b.i.d., Ara-C at 150 mg/kg (i.v.) q.d., or vehicle for 4 days. Six hours after the last administration, PB were collected. Total RNA was extracted from each PB using a QIAamp RNA Blood Mini Kit (Qiagen

Table 1. Kinase inhibitory profile and growth inhibition effects of FI-700 *in vitro*

Enzyme	Inhibitory activity at 1 μmol/L (%)
Tyrosine kinase	
FLT3	95
KIT	90
FMS	75
LYN	52
LCK	47
MET	25
EPHB2	23
BTK	14
TIE2	14
ALK	1
TRKB	1
ABL	0
EGFR	0
FES	0
Serine/threonine kinase	
GSK3β	15
Aurora A	11
MEK1	8
CDK2/Cyclin E	2

Cell line	IC_{50} value for growth (μmol/L)
Human leukemia cell line	
MV4;11	0.014
MOLM13	0.016
THP1	3.1
Kasumi-1	0.18
HL60	6.8
K562	5.2
MegO1	6.1
32D Transfectant	
32D (1 ng/mL IL-3)	>10
Wt-FLT3 (100 ng/mL FL)	0.780
FLT3/ITD	0.057
FLT3/D835Y	0.070

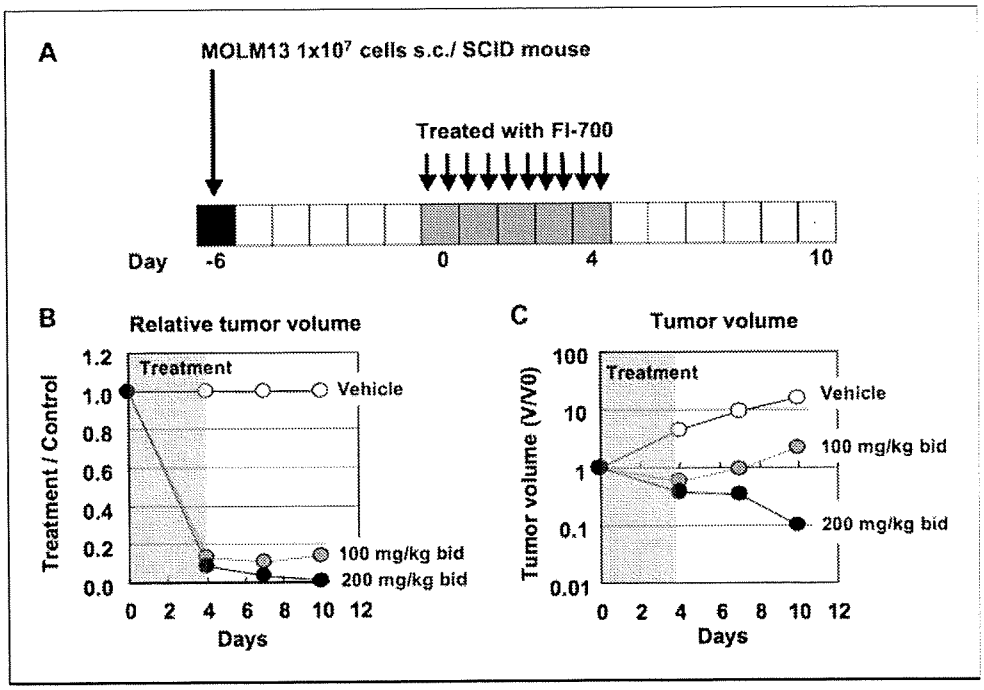

Fig. 2. Inhibitory effect on s.c. tumor in MOLM13/SCID-mice xenotransplant model. *A*, MOLM13 cells (1×10^7/mouse) were s.c. inoculated into SCID mice on day -6. FI-700 (100 or 200 mg/kg b.i.d.) or vehicle was given orally from days 0 to 4. *B*, the ratio of tumor volume in the treated to control mice. *C*, the relative tumor volume to the initial tumor volume on day 0 (V/V_0).

Inc.). cDNA was synthesized from each RNA using a random primer and Moloney murine leukemia virus reverse transcriptase (Super-Script II; Life Technologies) according to the manufacturer's recommendations. The expression level of the human FLT3 transcript was quantitated using a real-time fluorescence detection method on an ABI Prism 7000 sequence detection system (Applied Biosystems) as previously reported (13, 31). After the collection of PB, mice were sacrificed, and then femora and spleens were collected. BM cells were collected from femora and the total cell number from each femur was counted using a cell counter. In order to discriminate the FLT3/ITD-GFP-32D leukemia cells and normal BM cells, all collected cells were subjected to flow cytometry analysis after PE-conjugated anti-human FLT3 monoclonal antibody (DAKO) staining. In this flow cytometry analysis, GFP-positive cells were defined as residual leukemia in the femur. The weight of each collected spleen was measured.

Statistical analysis. Differences in continuous variables were analyzed with the unpaired *t* test for distribution between two groups. Survival probabilities were estimated by the Kaplan-Meier method, and differences in survival distributions were evaluated using the log-rank test. Differences in therapeutic effects were analyzed with the repeated-measures ANOVA method. These statistical analyses were done with StatView-J 5.0 (Abacus Concepts Inc.). For all analyses, the *P* values were two-tailed, and $P < 0.05$ was considered statistically significant.

Results

Selective kinase inhibition by FI-700. A novel small-molecule FLT3 kinase inhibitor, FI-700, was identified by screening the chemical libraries of Kyowa Hakko Kogyo.[5] The chemical structure of FI-700 is shown in Fig. 1A. FI-700 inhibited FLT3 kinase with an IC_{50} of 0.02 μmol/L for *in vitro* kinase assays. The selectivity of FI-700 was examined against a wide range of kinases (Table 1). Although FI-700 at 1 μmol/L showed >50% inhibition against KIT, FMS, or LYN kinases, it did not possess potent kinase inhibitory activity against ALK, TRKB, ABL, EGFR, FES, TIE2, MEK1 or CDK2.

Growth-inhibitory effects. To evaluate the selectivity and sensitivity of FI-700 in the cellular system, we examined its growth-inhibitory effects on FLT3-transfected 32D cells as well as on several human leukemia cell lines. Cells were treated with increasing concentrations of FI-700 for 72 h, and then viable cells were determined by the CellTiter^{96} Proliferation Assay. FI-700 selectively inhibited the growth of FLT3/ITD- and FLT3/D835Y-expressing 32D cells with IC_{50} values of 0.057 and 0.070 μmol/L, respectively, but not that of parental 32D cells with 1 ng/mL of IL-3 (Table 1). Notably, the IC_{50} value against Wt-FLT3-expressing 32D cells with 100 ng/mL of FL was more than 10 times lower than that against mutant FLT3-expressing 32D cells. Furthermore, growth inhibition against FLT3/ITD- and FLT3/D835Y-expressing 32D cells was cancelled by the addition of IL-3, indicating the selective inhibitory profile of FI-700 against constitutively active FLT3 kinases.

Consistent with the results from mutant FLT3-expressing 32D cells, FI-700 inhibited the growth of human leukemia cell lines harboring FLT3/ITD in a dose-dependent manner (Fig. 1B). As shown in Table 1, the IC_{50} values of FI-700 against MV4;11 and MOLM-13 were 0.014 and 0.016 μmol/L, respectively, whereas those against Wt-FLT3 expressing human leukemia were 10- to 100-fold higher. The IC_{50} value against Kasumi-1, which has an activating mutation in the *cKIT* gene, was 0.18 μmol/L, indicating the inhibitory potency of FI-700 against mutant cKIT kinase. In addition, the presence of FL did not affect the sensitivity of FI-700 against all human leukemia cell lines regardless of the expression of FLT3 protein (data not shown).

Inhibitory effects of FI-700 on FLT3 and downstream signals. MOLM13 cells were treated with increasing concentrations of FI-700 for 6 h. Cell lysates were subjected to Western blot analysis to detect the phosphorylation status of FLT3, signal transducers and activators of transcription 5 (STAT5), and mitogen-activated protein kinase (MAPK). FI-700 suppressed

[5] Manuscript in preparation.

Table 2. Treatment groups and dosing schedules used

	Dose (mg/kg)	Route	Schedule	T/C_{min} (on day)	Regression $V/V_{0\ min}$ (on day)	Body weight loss, g (on day)	Mortality
Control				1.00		0.6 (10)	0/5
FI-700	100	p.o.	b.i.d. × 5	0.10 (7)	0.571 (4)	0.7 (4, 7)	0/5
	200	p.o.	b.i.d. × 5	0.006 (10)	0.098 (10)	—	0/5
MLN-518	160	p.o.	b.i.d. × 5	0.48 (7)	—	—	0/5
PKC-412	400	p.o.	q.d. × 5	0.20 (7)	—	—	0/5

NOTE: FI-700 dosing at 100 and 200 mg/kg showed growth inhibition of tumors with T/C_{min} values of 0.10 (on day 7) and 0.006 (on day 10), respectively. Although the regrowth of MOLM-13 tumors was observed at 100 mg/kg after stopping FI-700 treatment, continuous regression of tumors was observed in mice treated with 200 mg/kg until day 10. No significant suppression of body weight gain or mortality was observed in the FI-700–treated group during the experiments. T/C_{min} values of MLN-518 and PKC-415 were 0.45 and 0.20 on day 7, respectively. However, tumor regression was not observed in either MLN-518- or PKC-412–treated mice.

the autophosphorylation of FLT3 as well as downstream molecules, such as STAT5 and MAPK, in a dose-dependent manner (Fig. 1C). Dephosphorylation of FLT3, STAT5, and MAPK was observed at concentrations above the IC_{50} value against MOLM-13 cells. Similar down-regulation of phosphorylated FLT3 and STAT5 was also observed in MV4;11, FLT3/ITD-, and FLT3/D835Y–expressing 32D cells (data not shown). These results indicated that FI-700 inhibited the growth of mutant FLT3-expressing cells by the dephosphorylation of constitutively active FLT3 kinase.

Cell cycle effects of FI-700. After treatment with increasing concentrations of FI-700 for 24 h, MOLM-13 cells exhibited an increase in the percentages of G_1 cells in comparison with controls. Simultaneously, a reciprocal reduction in the percentage of cells in the S-G_2 phase was observed. An apparent increase of sub-G_1 apoptotic cells was also observed at >0.10 μmol/L of FL-700 (Fig. 1D). These results indicated that dephosphorylation of FLT3 by FI-700 could induce cell cycle arrest and eventually cause apoptosis at concentrations above the IC_{50} value against MOLM-13 cells.

Antileukemia effect of FI-700 against s.c. MOLM-13 tumor xenografts in SCID mice. MOLM13 cells (1×10^7/mouse) were s.c. inoculated into SCID mice on day -6. The mean initial tumor volume on day 0 (V_0) was 149.2 ± 22.8 mm^3. The mice were orally given vehicle or FI-700. The ratio of tumor volume in the treated to control mice (T/C) and the relative tumor volume to V_0 (V/V_0) in each group were evaluated until day 10. In the MOLM-13 tumor xenograft model, oral administration of FI-700 at 100 or 200 mg/kg b.i.d. for 5 days showed a potent and significant antitumor effect in a dose-dependent manner (Fig. 2A). FI-700 dosing at 100 and 200 mg/kg showed growth inhibition of tumors with T/C minimum values (T/C_{min}) of 0.10 (on day 7) and 0.006 (on day 10), respectively (Fig. 2B). In addition, FI-700 dosing showed tumor regression, giving V/V_0 (0.571) on day 7 at 100 mg/kg and V/V_0 (0.098) on day 10 at 200 mg/kg, respectively. Although the regrowth of MOLM-13 tumors was observed at 100 mg/kg after stopping FI-700 treatment, continuous regression of tumors was observed in mice treated with 200 mg/kg until day 10 (Fig. 2C). No significant suppression of body weight gain or mortality was observed in the FI-700–treated group during the experiments (Table 2). On the other hand, MLN-518 and PKC-412 at the maximum tolerated dose on day 7 showed growth inhibition of tumors with T/C_{min} of 0.45 and 0.20, respectively. However, no tumor regression was observed both in MLN-518- or PKC-412–treated animals (Table 2).

In the other xenograft model, in which MOLM-13 cells were i.v. inoculated into SCID mice, FI-700–treated mice showed a significantly longer survival time than Ara-C–treated mice (P = 0.019, log-rank test; Fig. 3).

Inhibitory effects of FI-700 on leukemia cells in a syngeneic transplantation model. FLT3/ITD-GFP-32D cells were i.v. inoculated into syngeneic C3H/Hej mice, and FI-700, Ara-C, or vehicle was administered to the mice 11 days after inoculation. In this model, the *in vivo* efficacy of FI-700 against FLT3/ITD-expressing cells was compared with the conventional antileukemic agent Ara-C (Fig. 4A). By quantitating the human FLT3 transcripts, we first compared the number of FLT3/ITD-GFP-32D cells in PB between before and after treatment with each drug. At the 7th day after inoculation, mean FLT3 transcript levels were 24.4 ± 6.7, 157.3 ± 139.4, and 42 ± 12.5 copy/μgRNA in vehicle-, FI-700-, and Ara-C–treated mice, respectively. In all vehicle-treated mice, FLT3 transcript levels increased, and the mean FLT3 transcript level on day 13 was

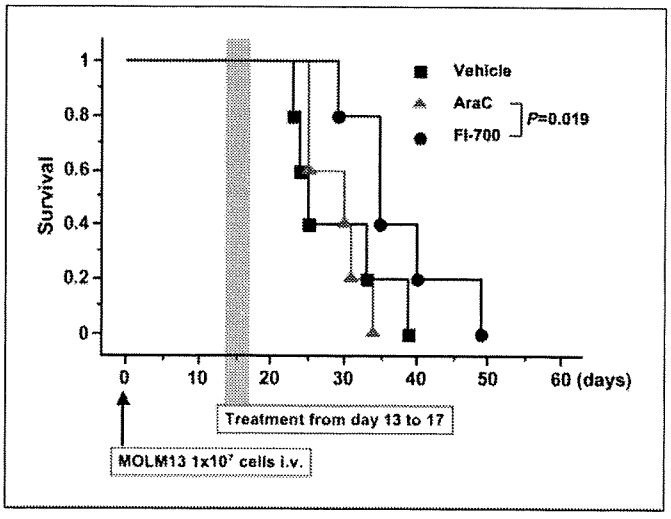

Fig. 3. Inhibition effect on i.v. tumor in MOLM13/SCID mice xenotransplant model. MOLM-13 cells were i.v. inoculated into SCID mice. From the 13th day after inoculation, mice were given FI-700 at 200 mg/kg (p.o.) b.i.d., Ara-C at 75 mg/kg (i.v.) b.i.d., or vehicle for 5 d. FI-700–treated mice showed a significantly longer survival time than Ara-C–treated mice (P = 0.019, log-rank test).

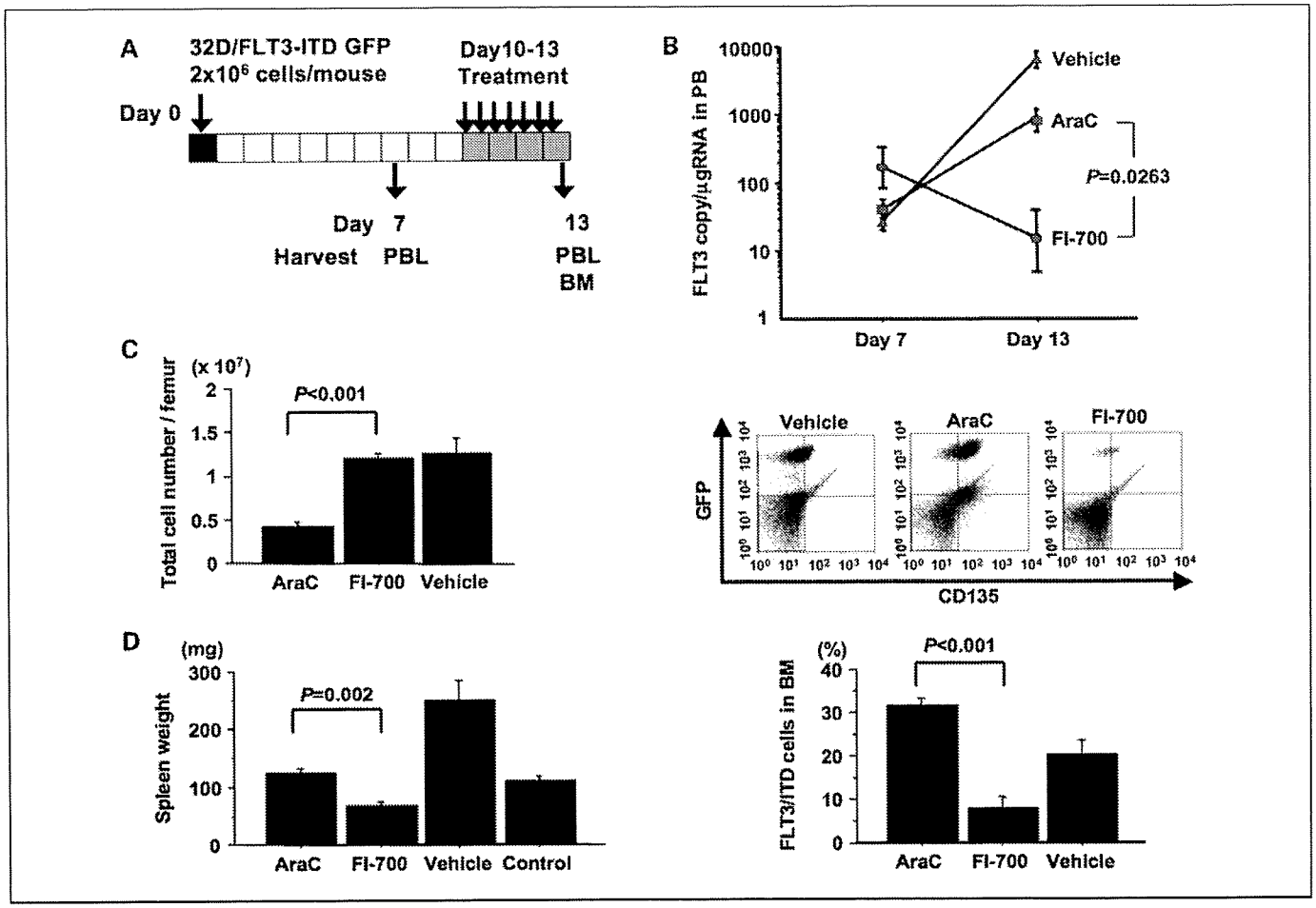

Fig. 4. Inhibition effects on FLT3/ITD-GFP-32D leukemic cells in C3H-Hej mice syngeneic transplantation model. *A*, C3H-Hej mice were inoculated with 2×10^6 of FLT3/ITD-GFP-32D cells on day 0. From the 10th day after inoculation, mice were given FI-700 at 200 mg/kg (p.o.) b.i.d., Ara-C at 150 mg/kg (i.v.) q.d., or vehicle for 4 d. PB was collected from each mouse on days 7 and 13. BM was collected on day 13. *B*, human FLT3 transcripts in PB were quantitated by a real-time fluorescence detection method. FI-700 treatment significantly represses the expansion of FLT3/ITD-GFP-32D cells compared with Ara-C treatment ($P = 0.0263$; *top*). The percentage of residual BM FLT3/ITD-GFP-32D cells in the femur was compared among vehicle-, FI-700-, and Ara-C – treated mice using flow cytometry. Representative results of flow cytometry (*middle*). Mean percentage of residual FLT3/ITD-GFP-32D cells were decreased to 8.0 ± 2.4% in the FI-700– treated group, whereas that of Ara-C – treated mice was 31.6 ± 1.6% ($P = 0.0143$; *bottom*). *C*, mean total cell numbers in the femur following treatment. The total number of nuclear cells in the BM of Ara-C – treated mice was significantly decreased when compared with that of FI-700– treated mice [$(0.42 \pm 0.06) \times 10^7$ and $(1.19 \pm 0.06) \times 10^7$ cells/femur, respectively; $P < 0.0001$], whereas the total cell number of FI-700– treated mice was the same as that of healthy control mice [$(1.53 \pm 0.23) \times 10^7$ cells/femur]. *D*, mean spleen weights of each treated mouse. The mean spleen weight of FI-700– treated mice (67.1 ± 4.9 mg) was significantly lighter than that of Ara-C – or vehicle – treated mice (122.2 ± 9.1 mg; $P = 0.0017$; 249.7 ± 33.9; $P = 0.0021$, respectively).

5,869.6 ± 1,640 copy/μgRNA. In contrast, FI-700 treatment repressed the expansion of FLT3/ITD-GFP-32D cells as the decrease of FLT3 transcript levels was observed in all mice, and the mean FLT3 transcript level was 13.5 ± 10.6 copy/μgRNA on day 13. The increased level of FLT3 transcripts in all Ara-C–treated mice was lower than that in vehicle-treated mice, although the effect of Ara-C treatment was limited as the mean FLT3 transcript level was 882.7 ± 305.5 copy/μgRNA on day 13. These results showed that the repressive effects of FI-700 on the expansion of FLT3/ITD-GFP-32D cells were significantly stronger than those by Ara-C ($P = 0.0263$, repeated-measures ANOVA; Fig. 4B). We next compared the percentage of residual

Table 3. Clinical characteristics of each case

Case	French-American-British classification	Age (y)	Karyotype
Wt-1	M_2	55	46,XX, t(8;21)(q22;q22)
Wt-2	M_1	54	46,XY
KDM	M_3	41	46,XX, t(15;17)(q22;q21)
ITD-1	M_0	45	46,XX
ITD-2	M_1	50	46,XY

BM FLT3/ITD-GFP-32D cells in the femur between FI-700 and Ara-C treatment using flow cytometry analysis. As shown in Fig. 4B, the mean percentage of FLT3/ITD-GFP-32D cells in BM was 20.2 ± 3.4% in vehicle-treated mice. In contrast, the mean percentage of FLT3/ITD-GFP-32D cells was decreased to 8.0 ± 2.4% in the FI-700–treated group, whereas that of Ara-C–treated mice was 31.6 ± 1.6% (P = 0.0143; Fig. 4B). Notably, the total number of nuclear cells in the BM of Ara-C–treated mice was significantly decreased when compared with that of FI-700–treated mice [$(0.42 \pm 0.06) \times 10^7$ and $(1.19 \pm 0.06) \times 10^7$ cells/femur, respectively, $P < 0.0001$], whereas the total cell number of FI-700–treated mice was the same as that of healthy control mice [$(1.53 \pm 0.23) \times 10^7$ cells/femur; Fig. 4C]. Furthermore, the mean spleen weight of FI-700–treated mice (67.1 ± 4.9 mg) was significantly lighter than that of Ara-C- or vehicle-treated mice (122.2 ± 9.1 mg; P = 0.0017; 249.7 ± 33.9; P = 0.0021, respectively; Fig. 4D). These results indicate that FI-700 has the potential to eradicate leukemia cells harboring FLT3 mutations without severe BM suppression.

Growth-inhibitory effects on primary AML cells. We finally analyzed the *in vitro* growth-inhibitory effects of FI-700 on five primary AML cells consisting of two Wt-FLT3, two FLT3/ITD, and one FLT3/D835Y case. The characteristics of these AML cases are shown in Table 3. Because the viability of primary AML cells drastically decreased even when cultured without FI-700 for >3 days, we evaluated the viable AML cells after treatment with or without 100 nmol/L of FI-700 for 48 h. FI-700 did not affect the growth of two AML cells with Wt-FLT3, whereas it reduced the growth of all FLT3/ITD- or FLT3/D835Y-AML cells (Fig. 5). Furthermore, the addition of FL (100 ng/mL) did not affect the growth-inhibitory activity of FI-700 against primary AML cells regardless of *FLT3* mutations (Fig. 5).

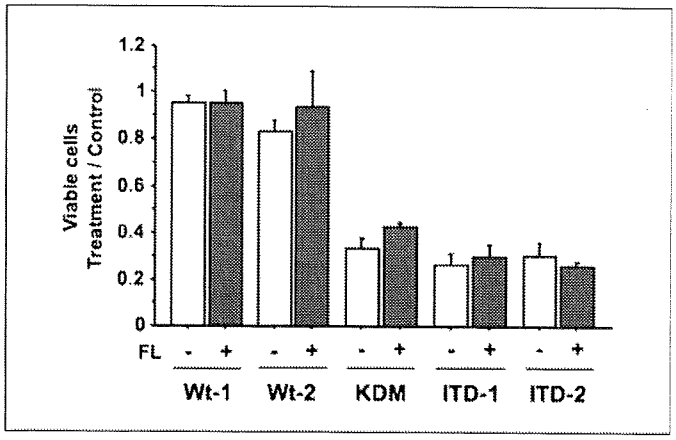

Fig. 5. Inhibitory effects on primary human AML cells. Growth inhibition effects of FI-700 at 100 nmol/L for 48 h on five primary AML cells. FI-700 did not affect the growth of two AML cells with Wt-FLT3, although it reduced the growth of all FLT3/ITD- or FLT3/D835Y-AML cells (*white columns*). The addition of FL (100 ng/mL) did not affect the growth inhibition activity of FI-700 against primary AML cells regardless of *FLT3* mutations (*gray columns*).

Discussion

FLT3 kinase is thought to be a promising therapeutic target for acute leukemia, and it is highly expected that the development of FLT3-selective small-molecule tyrosine kinase inhibitors will make a more efficacious therapeutic strategy for leukemia therapy. To date, several tyrosine kinase inhibitors have been shown to have the potency to inhibit the FLT3 kinase, whereas no FLT3 kinase–specific inhibitor has been approved as an antileukemia agent. FI-700 has been discovered and developed as an orally available and selective kinase inhibitor against FLT3. In this study, we evaluated the antileukemia activity and proof of concept of FI-700 as a FLT3 kinase inhibitor both *in vitro* and *in vivo*.

FI-700 showed potent and selective inhibitory activity against FLT3 kinase by *in vitro* kinase assays. In addition, it showed little inhibitory activity against a wide variety of tyrosine and serine/threonine kinases. This kinase inhibition profile was also confirmed by the cellular system as potent and selective growth inhibition against both FLT3/ITD- and FLT3/D835Y-carrying cells. It was further shown that growth inhibition by FI-700 was dependent on the dephosphorylation of constitutively active mutant FLT3 kinases as well as STAT5 and MAPK. In addition, cell cycle analysis revealed that FI-700 induced G_1 arrest over the concentration of IC_{50} value against mutant FLT3-expressing leukemia cells, resulting in apoptosis. On the other hand, its potency against constitutively active FLT3 kinase was >10 times higher than Wt-FLT3 kinase. Because hematopoietic progenitors express Wt-FLT3, the lower potency against it seemed an advantage to avoid BM suppression in clinical use. These characteristics of FI-700 obtained from *in vitro* analyses might be favorable characteristics of FI-700 for patients with leukemia.

To evaluate the antileukemia efficacy of FI-700 *in vivo*, we employed two distinct s.c. or i.v. inoculated xenograft model. In the s.c. inoculated model, oral treatment of mice with FI-700 for 5 days showed tumor regression without body weight loss. In this model, whereas tumor regression was transient and tumor regrowth was observed after stopping FI-700 at 100 mg/kg, continuous tumor regression was observed in mice treated with 200 mg/kg, suggesting the curative potency of FI-700. When we compared the efficacy of FI-700 with those of MLN-518 or PKC-412 at the maximum tolerated dose, oral treatment of FI-700 showed superior antileukemia activity in the MOLM-13 inoculated model. Furthermore, in the i.v.-inoculated model, 5-day treatment with FI-700 prolonged the life span of leukemia-inoculated mice and its efficacy was more potent than that of conventional therapeutics, Ara-C. However, all mice eventually died even in the FI-700–treated group, indicating that longer treatment with FI-700 was necessary for the complete eradication of leukemia cells. Our preliminary study showed that 14-day treatment with FI-700 at 200 mg/kg b.i.d. could prolong the survival compared with 5-day treatment, suggesting that longer treatment with FI-700 might improve the efficacy of the drug. Therefore, a longer treatment schedule could be necessary to provide a cure for leukemia.

The efficacy of FI-700 was further confirmed in the other syngeneic i.v. transplanted model. In this model, we compared the potency against leukemic FLT3/ITD-expressing cells between FI-700 and Ara-C. As shown in Fig. 4, it was quantitatively shown that FI-700 significantly eradicated more FLT3/ITD-expressing cells both from PB and BM compared with Ara-C. The most important finding was that BM suppression by FI-700 was significantly less than that by Ara-C. This lower BM suppression might depend on the selective kinase inhibition profile of FI-700. The treatment schedule of Ara-C used here almost corresponds with the high-dose Ara-C

regimen, which is clinically used for patients with leukemia. Although it remains unclear whether high-dose chemotherapy, such as the high-dose Ara-C regimen, conquers the adverse effect of *FLT3* mutations, two large-scale studies raised the possibility that therapeutic regimens employing high-dose Ara-C might contribute towards a better outcome in patients with AML (32, 33). The high-dose Ara-C regimen, a dose-intensified regimen, is an established treatment strategy both for newly diagnosed and relapsed or refractory acute leukemia patients, whereas severe BM suppression is known to be an unavoidable adverse effect of this regimen (34). In the present mice model, BM suppression was consistently induced by Ara-C treatment, although the antileukemia effect was limited. Therefore, the selective antileukemia activity of FI-700 against FLT3/ITD-expressing cells without severe BM suppression could be ideal for the treatment of patients with leukemia.

It has been suggested that AML is the consequence of two broad complementation classes of mutations: those that confer a proliferative and/or survival advantage to hematopoietic progenitors (class I) including activating mutations in tyrosine kinases or their downstream effectors, and those that impair hematopoietic differentiation and confer properties of self-renewal (class II) including rearrangements or point mutations of core-binding factor genes and *PML-RARA* (35). *FLT3* mutations have been frequently found in AML patients with *PML-RARA* translocation, whereas they have also been preferentially found in AML patients with a normal karyotype, suggesting that additional genetic alterations are involved in the pathogenesis of AML with *FLT3* mutations (8). Therefore, it is thought to be difficult to cure leukemia by monotherapy with a FLT3 inhibitor. This is also supported by recent results from clinical trials of potent FLT3 inhibitors, such as MLN-518, PKC-412, or CEP-701. Although FI-700 showed a growth-inhibitory effect on primary AML cells with *FLT3* mutations, combination effects with conventional chemotherapeutic agents should be further evaluated.

Acknowledgments

We thank Manami Kira for secretarial assistance.

References

1. Rosnet O, Schiff C, Pebusque MJ, et al. Human FLT3/FLK2 gene: cDNA cloning and expression in hematopoietic cells. Blood 1993;82:1110–9.
2. Lyman SD, James L, Zappone J, Sleath PR, Beckmann MP, Bird T. Characterization of the protein encoded by the flt3 (flk2) receptor-like tyrosine kinase gene. Oncogene 1993;8:815–22.
3. Matthews W, Jordan CT, Wiegand GW, Pardoll D, Lemischka IR. A receptor tyrosine kinase specific to hematopoietic stem and progenitor cell-enriched populations. Cell 1991;65:1143–52.
4. Robertson SC, Tynan J, Donoghue DJ. RTK mutations and human syndromes: when good receptors turn bad. Trends Genet 2000;16:265–71.
5. Nakao M, Yokota S, Iwai T, et al. Internal tandem duplication of the flt3 gene found in acute myeloid leukemia. Leukemia 1996;10:1911–8.
6. Kiyoi H, Towatari M, Yokota S, et al. Internal tandem duplication of the FLT3 gene is a novel modality of elongation mutation which causes constitutive activation of the product. Leukemia 1998;12:1333–7.
7. Yamamoto Y, Kiyoi H, Nakano Y, et al. Activating mutation of D835 within the activation loop of FLT3 in human hematologic malignancies. Blood 2001;97:2434–9.
8. Kiyoi H, Yanada M, Ozeki K. Clinical significance of FLT3 in leukemia. Int J Hematol 2005;82:85–92.
9. Taketani T, Taki T, Sugita K, et al. FLT3 mutations in the activation loop of tyrosine kinase domain are frequently found in infant ALL with MLL rearrangements and pediatric ALL with hyperdiploidy. Blood 2004;103:1085–8.
10. Armstrong SA, Kung AL, Mabon ME, et al. Inhibition of FLT3 in MLL. Validation of a therapeutic target identified by gene expression based classification. Cancer Cell 2003;3:173–83.
11. Armstrong SA, Mabon ME, Silverman LB, et al. FLT3 mutations in childhood acute lymphoblastic leukemia. Blood 2004;103:3544–6.
12. Armstrong SA, Staunton JE, Silverman LB, et al. MLL translocations specify a distinct gene expression profile that distinguishes a unique leukemia. Nat Genet 2002;30:41–7.
13. Ozeki K, Kiyoi H, Hirose Y, et al. Biologic and clinical significance of the FLT3 transcript level in acute myeloid leukemia. Blood 2004;103:1901–8.
14. Gale RE, Hills R, Kottaridis PD, et al. No evidence that FLT3 status should be considered as an indicator for transplantation in acute myeloid leukemia (AML): an analysis of 1135 patients, excluding acute promyelocytic leukemia, from the UK MRC AML10 and 12 trials. Blood 2005;106:3658–65.
15. Stirewalt DL, Radich JP. The role of FLT3 in haematopoietic malignancies. Nat Rev Cancer 2003;3:650–65.
16. Gilliland DG, Griffin JD. The roles of FLT3 in hematopoiesis and leukemia. Blood 2002;100:1532–42.
17. Stone RM, DeAngelo DJ, Klimek V, et al. Patients with acute myeloid leukemia and an activating mutation in FLT3 respond to a small-molecule FLT3 tyrosine kinase inhibitor, PKC412. Blood 2005;105:54–60.
18. Knapper S, Burnett AK, Littlewood T, et al. A phase 2 trial of the FLT3 inhibitor lestaurtinib (CEP701) as first line treatment for older patients with acute myeloid leukemia not considered fit for intensive chemotherapy. Blood 2006;108:3262–70.
19. Fiedler W, Serve H, Dohner H, et al. A phase 1 study of SU11248 in the treatment of patients with refractory or resistant acute myeloid leukemia (AML) or not amenable to conventional therapy for the disease. Blood 2005;105:986–93.
20. DeAngelo DJ, Stone RM, Heaney ML, et al. Phase 1 clinical results with tandutinib (MLN518), a novel FLT3 antagonist, in patients with acute myelogenous leukemia or high-risk myelodysplastic syndrome: safety, pharmacokinetics, and pharmacodynamics. Blood 2006;108:3674–81.
21. Kiyoi H, Naoe T. Biology, clinical relevance, and molecularly targeted therapy in acute leukemia with FLT3 mutation. Int J Hematol 2006;83:301–8.
22. Levis M, Small D. FLT3 tyrosine kinase inhibitors. Int J Hematol 2005;82:100–7.
23. Davies SP, Reddy H, Caivano M, Cohen P. Specificity and mechanism of action of some commonly used protein kinase inhibitors. Biochem J 2000;351:95–105.
24. Kiyoi H, Ohno R, Ueda R, Saito H, Naoe T. Mechanism of constitutive activation of FLT3 with internal tandem duplication in the juxtamembrane domain. Oncogene 2002;21:2555–63.
25. Zhao M, Kiyoi H, Yamamoto Y, et al. *In vivo* treatment of mutant FLT3-transformed murine leukemia with a tyrosine kinase inhibitor. Leukemia 2000;14:374–8.
26. Kiyoi H, Naoe T, Nakano Y, et al. Prognostic implication of FLT3 and N-RAS gene mutations in acute myeloid leukemia. Blood 1999;93:3074–80.
27. Kiyoi H, Naoe T, Yokota S, et al. Internal tandem duplication of FLT3 associated with leukocytosis in acute promyelocytic leukemia. Leukemia Study Group of the Ministry of Health and Welfare (Kohseisho). Leukemia 1997;11:1447–52.
28. Minami Y, Yamamoto K, Kiyoi H, Ueda R, Saito H, Naoe T. Different antiapoptotic pathways between wild-type and mutated FLT3: insights into therapeutic targets in leukemia. Blood 2003;102:2969–75.
29. Levis M, Allebach J, Tse KF, et al. A FLT3-targeted tyrosine kinase inhibitor is cytotoxic to leukemia cells *in vitro* and *in vivo*. Blood 2002;99:3885–91.
30. Kelly LM, Yu JC, Boulton CL, et al. CT53518, a novel selective FLT3 antagonist for the treatment of acute myelogenous leukemia (AML). Cancer Cell 2002;1:421–32.
31. Iwai M, Kiyoi H, Ozeki K, et al. Expression and methylation status of the FHIT gene in acute myeloid leukemia and myelodysplastic syndrome. Leukemia 2005;19:1367–75.
32. Thiede C, Steudel C, Mohr B, et al. Analysis of FLT3-activating mutations in 979 patients with acute myelogenous leukemia: association with FAB subtypes and identification of subgroups with poor prognosis. Blood 2002;99:4326–35.
33. Schnittger S, Schoch C, Dugas M, et al. Analysis of FLT3 length mutations in 1003 patients with acute myeloid leukemia: correlation to cytogenetics, FAB subtype, and prognosis in the AMLCG study and usefulness as a marker for the detection of minimal residual disease. Blood 2002;100:59–66.
34. Mayer RJ, Davis RB, Schiffer CA, et al. Intensive postremission chemotherapy in adults with acute myeloid leukemia. Cancer and Leukemia Group B. N Engl J Med 1994;331:896–903.
35. Speck NA, Gilliland DG. Core-binding factors in haematopoiesis and leukaemia. Nat Rev Cancer 2002;2:502–13.

(Figures 1c and d). The re-evaluation of G-banding results revealed hardly visible small paired particles in some of the metaphases, which may be small dmins (Figure 1e). Small extrachromosomal amplicons are described either as episomes (<1 Mb in size) or dmins (usually several Mb), depending on visualization under the microscope. Array CGH makes it easier to detect these small structures and reports of other amplicons in leukemia can be expected in the near future.

In conclusion, although mutations in *FLT3*, *NPM1* or other genes are known minimal residual disease follow up-markers in karyotypically normal AML,[1] alterations detected by aCGH may also serve as markers, especially in cases where mutations are not detected. Furthermore, the altered genes, we detected using oligonucleotide aCGH may be potential oncogenes or tumor suppressors contributing to leukemogenesis.

Acknowledgements

This work was supported by grants from the Foundation for the Finnish Cancer Institute and Helsinki University Central Hospital research funds.

A Tyybäkinoja[1], E Elonen[2], K Piippo[1], K Porkka[3] and S Knuutila[1]
[1]*Department of Pathology, Haartman Institute and HUSLAB, University of Helsinki and Helsinki University Central Hospital, Helsinki, Finland;*
[2]*Department of Medicine, Division of Hematology, Helsinki University Central Hospital, Helsinki, Finland and*
[3]*Hematology Research Unit, Biomedicum Helsinki, Helsinki, Finland*
E-mail: sakari.knuutila@helsinki.fi

References

1 Mrozek K, Marcucci G, Paschka P, Whitman SP, Bloomfield CD. Clinical relevance of mutations and gene-expression changes in adult acute myeloid leukemia with normal cytogenetics: are we ready for a prognostically prioritized molecular classification? *Blood* 2007; **109**: 431–448.
2 Dalley CD, Neat MJ, Foot NJ, Burridge M, Byrne L, Amess JA *et al.* Comparative genomic hybridization and multiplex-fluorescence *in situ* hybridization: an appraisal in elderly patients with acute myelogenous leukemia. *Hematol J* 2002; **3**: 290–298.
3 Frohling S, Skelin S, Liebisch C, Scholl C, Schlenk RF, Dohner H *et al.* Comparison of cytogenetic and molecular cytogenetic detection of chromosome abnormalities in 240 consecutive adult patients with acute myeloid leukemia. *J Clin Oncol* 2002; **20**: 2480–2485.
4 Paulsson K, Heidenblad M, Strombeck B, Staaf J, Jonsson G, Borg A *et al.* High-resolution genome-wide array-based comparative genome hybridization reveals cryptic chromosome changes in AML and MDS cases with trisomy 8 as the sole cytogenetic aberration. *Leukemia* 2006; **20**: 840–846.
5 Rucker FG, Bullinger L, Schwaenen C, Lipka DB, Wessendorf S, Frohling S *et al.* Disclosure of candidate genes in acute myeloid leukemia with complex karyotypes using microarray-based molecular characterization. *J Clin Oncol* 2006; **24**: 3887–3894.
6 Tyybakinoja A, Saarinen-Pihkala U, Elonen E, Knuutila S. Amplified, lost, and fused genes in 11q23–25 amplicon in acute myeloid leukemia, an array-CGH study. *Genes Chromosomes Cancer* 2006; **45**: 257–264.
7 Sato Y, Suto Y, Pietenpol J, Golub TR, Gilliland DG, Davis EM *et al.* TEL and KIP1 define the smallest region of deletions on 12p13 in hematopoietic malignancies. *Blood* 1995; **86**: 1525–1533.
8 Storlazzi CT, Fioretos T, Surace C, Lonoce A, Mastrorilli A, Strombeck B *et al.* MYC-containing double minutes in hematologic malignancies: evidence in favor of the episome model and exclusion of MYC as the target gene. *Hum Mol Genet* 2006; **15**: 933–942.

Supplementary Information accompanies the paper on the Leukemia website (http://www.nature.com/leu)

JAK3 mutations occur in acute megakaryoblastic leukemia both in Down syndrome children and non-Down syndrome adults

Leukemia (2007) **21**, 574–576. doi:10.1038/sj.leu.2404527;
published online 25 January 2007

Acute myeloid leukemia (AML) is thought to be the consequence of two broad complementation classes of mutations: those that confer a proliferative and/or survival advantage to hematopoietic progenitors, and those that impair hematopoietic differentiation and confer properties of self-renewal.[1] AML in Down syndrome (DS) children shows unique characteristics of the predominance of acute megakaryoblastic leukemia (AMKL) and a preceding history of transient myeloproliferative disorder (TMD), whose blasts are morphologically and phenotypically indistinguishable from those of AMKL. TMD develops in about 10% of DS infants and resolves spontaneously in most cases, while 20% of TMD cases develop AMKL within 3 years. Somatic mutations of the *GATA1* gene are reportedly associated with AMKL in DS children.[2] In addition, subsequent reports demonstrated that *GATA1* mutations are an early event in DS leukemogenesis and contribute to the pathogenesis of both TMD and AMKL, suggesting that the acquisition of additional genetic alterations might be necessary for progression from TMD to AMKL;[3] however, it remains unclear which mutations are involved in the progression of TMD to AMKL. Furthermore, little is known about which genetic alterations are involved in the pathogenesis of non-DS AMKL. Recently, Walters *et al.*[4] reported activating mutations of the *JAK3* gene in each of 16 non-DS and three DS AMKL patients as well as an AMKL cell line CMK derived from a DS AMKL patient. These mutations consisted of A572V and V722I substitutions in the JH2 pseudokinase domain, and a P132T substitution in the JH6 domain of the receptor-binding domain. Although the mutated positions were different, all mutated JAK3 products were constitutively activated and conferred autonomous proliferation of Ba/F3 cells. These results suggested that activating *JAK3* mutations involved in the pathogenesis of AMKL both with and without DS, whereas it remains unclear how *JAK3* mutations cooperate with other genetic alterations during leukemogenesis. In this study, we analyzed *JAK3* mutations in non-DS adults with AMKL and DS children with AMKL or TMD in comparison with mutations in *GATA1*, *p53*, *FLT3* and *N-RAS* genes.

The study population included eight non-DS adults with AMKL, and 11 AMKL and two TMD children with DS. The diagnosis of AMKL and TMD was based on morphology,

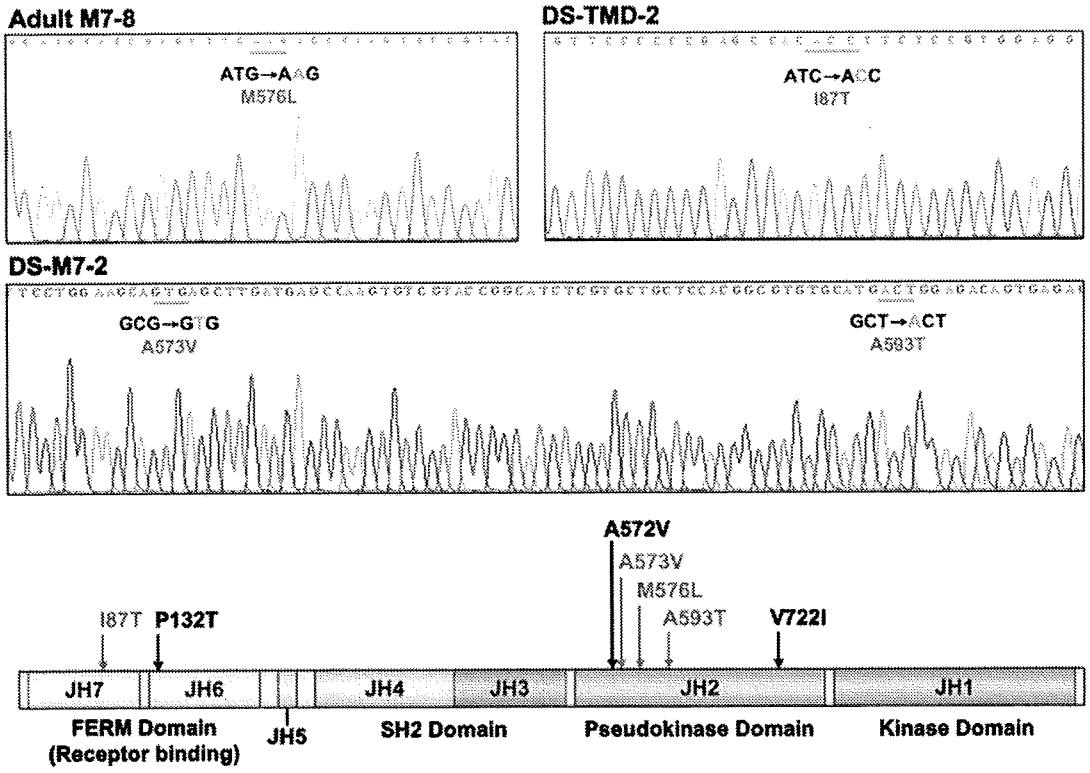

Figure 1 *JAK3* mutations found in AMKL and TMD patients. We found four novel *JAK3* mutations (I87T, A573V, M576L and A593T indicated by red letters) in AMKL and TMD patients. A573V and A593T mutations were found in the same allele. All *JAK3* mutations including those previously found by Walters *et al.* (P132T, A572T and V722I indicated by black letters) were located in the JH2 pseudokinase domain or the receptor-binding domain.

Table 1 Mutations of *JAK3, GATA1, p53, FLT3* and *N-RAS* genes in AMKL and TMD patients

UPN	*Sex*	*JAK3*	*GATA1*	*p53*	*FLT3*	*N-RAS*
Adult M7-1	M	Wild	Wild	Wild	Wild	Wild
Adult M7-2	M	Wild	Wild	Mutation	Wild	Wild
Adult M7-3	M	Wild	Wild	Wild	Wild	Wild
Adult M7-4	M	Wild	Wild	Wild	Wild	Wild
Adult M7-5	F	Wild	Wild	Wild	Wild	Wild
Adult M7-6	M	Wild	Wild	Mutation	Wild	Wild
Adult M7-7	F	M576L	Wild	Mutation	Wild	Wild
Adult M7-8	F	Wild	Wild	Wild	Wild	Wild
DS-M7-1	M	Wild	Mutation	Wild	Wild	Wild
DS-M7-2	M	A573V and A593T	Mutation	Wild	Wild	Wild
DS-M7-3	F	Wild	Mutation	Mutation	Wild	Wild
DS-M7-4	F	Wild	Mutation	Wild	Wild	Wild
DS-M7-5	F	Wild	Mutation	Wild	Wild	Wild
DS-M7-6	F	Wild	Mutation	Wild	Wild	Wild
DS-M7-7	F	Wild	Mutation	Wild	Wild	Wild
DS-M7-8	F	Wild	Mutation	Wild	Wild	Wild
DS-M7-9	M	Wild	Mutation	Wild	Wild	Wild
DS-M7-10	F	Wild	Mutation	Mutation	Wild	Wild
DS-M7-11	M	Wild	Mutation	Wild	Wild	Wild
DS-TMD-1	F	Wild	Mutation	Wild	Wild	Wild
DS-TMD-2	M	I87T	Mutation	Wild	Wild	Wild

JAK3 mutations were found in three patients. In DS-M7-2, two distinct *JAK3* mutations were found in the same allele. *GATA1* mutations were found in all AMKL and TMD patients with DS, but not in adult non-DS AMKL patients.

histopathology, the expression of leukocyte differentiation antigens and/or the French–American–British (FAB) classification. The diagnosis of DS was confirmed by conventional cytogenetic analysis. Bone marrow (BM) samples were obtained from patients with AMKL and TMD at diagnosis after obtaining informed consent for banking and molecular analyses from all adult patients or parents of children. High-molecular-weight DNA was extracted from the samples by the standard method. For screening of *JAK3* mutations, we amplified genomic DNA corresponding to all 23 exons of the *JAK3* gene by polymerase

chain reaction (PCR) using 19 primer pairs. Amplified products were subjected to denaturing HPLC (DHPLC) analysis using the WAVE Maker System (Transgenomic Inc., San Jose, CA, USA). DHPLC gradients and temperatures were determined using WAVE Maker System software. When heterozygous profiles were identified by visual inspection of the chromatograms, amplified products were cloned into pGEM-T Easy vector (Promega, Madison, WI, USA) and sequenced on a DNA sequencer (310; Applied Biosystems, Foster City, CA, USA) using a BigDye terminator cycle-sequencing kit (Applied Biosystems). *GATA1* mutations of exon 2, *FLT3* mutations, *N-RAS* mutations of codons 12, 13 and 61 and *p53* mutations of exons 5–8 were examined as previously reported.[5,6]

Mutations of *JAK3* were found in each adult with non-DS AMKL, DS AMKL and DS TMD; a M576L substitution in the JH2 pseudokinase domain in adult non-DS AMKL (UPN: adult M7-8); A573V and A593T substitutions in DS AMKL (UPN: DS-M7-2) and an I87T substitution in the JH7 domain of the receptor-binding domain in DS TMD (UPN: DS-TMD-2) (Figure 1). In the DS-M7-2 patient, A573V and A593T substitutions were found in the same allele. We therefore sequenced 20 independent clones to examine for the existence of single mutant alleles, and all mutant alleles had both mutations, indicating that most leukemia cells had both mutations at diagnosis. *GATA1* mutations were observed in all DS AMKL and DS TMD patients, but not in non-DS AMKL adults. *p53* Mutations were found in three of eight non-DS AMKL and two of eleven DS AMKL patients, but not in two TMD patients. No *FLT3* and *N-RAS* mutations were found in any AMKL and TMD patients (Table 1).

In this study, we found four types of *JAK3* mutations in AMKL and TMD patients. These mutations were different from those previously found in AMKL patients and the megakaryoblastic cell line CMK, while it was notable that all *JAK3* mutations uniformly occurred in the pseudokinase domain or receptor-binding domain. JAK3 consists of seven Janus homology (JH) domains, JH1–JH7. The JH2 pseudokinase domain lies adjacent to the JH1 C-terminal kinase domain. Although the pseudokinase domain itself lacks catalytic activity, it has been demonstrated that a number of mutations in this domain derived from severe combined immunodeficiency (SCID) patients abrogate kinase activity indicating its essential regulatory activity for the kinase domain.[7] Therefore, it is an important question why *JAK3* mutations identified in AMKL are activating mutations in contrast to loss-of-function mutations identified in SCID patients. Walters *et al.*[4] speculated the possible autoinhibitory function of the pseudokinase domain against the kinase domain by structural modeling analysis. Since the activating mutation in the JH2 pseudokinase domain of JAK2 ($JAK2^{V617F}$) was preferentially found in myeloproliferative disorders,[8] *JAK3* mutations in this region might be involved in the proliferation mechanism of megakaryoblastic cells. However, in contrast to the *JAK2* mutation, mutations of *JAK3* were observed in a variety of residues within the JH2 pseudokinase domain. Further analysis is therefore necessary to examine whether each *JAK3* mutation identified in this study is an activating mutation. The important aspect of this study was the *JAK3* mutation in TMD patients. This I87T mutation was found in the JH7 domain of the receptor-binding domain. N-terminal JH5–JH7 domains of JAK3, which has homology to the band four-point-one, ezrin, radixin, moesin (FERM) domain-containing proteins, mediates binding to the common γ-subunit (γ_c), which is a common receptor subunit for IL-2, IL-4, IL-7, IL-9, IL-15 and IL-21 cytokines.[7] Since mutations in this domain identified in SCID patients are also demonstrated to abrogate the binding capacity to γ_c and catalytic activity, it is necessary to examine whether the I87T mutation is an activating mutation like the P132T mutation found in non-DS AMKL patients. The fact that the *JAK3* mutation was found in a TMD patient indicated that it is an early event during the development of AMKL in DS patients, whereas its pathological significance should be carefully examined. Furthermore, since we could not find any relationship between the *JAK3* mutation and *GATA1*, *p53*, *FLT3* and *N-RAS* mutations, it should be further examined which genetic alterations collaborate with *JAK3* mutations, and how *JAK3* mutations are involved in the development and/or progression of AMKL.

Acknowledgements

We thank Ms Manami Kira for secretarial assistance. This work was supported by Grants-in-Aid from the National Institute of Biomedical Innovation, the Ministry of Health, Labor and Welfare and the Scientific Research of the Ministry of Education, Culture, Sports, Science and Technology, Japan.

H Kiyoi[1], S Yamaji[1], S Kojima[2] and T Naoe[3]
[1]*Department of Infectious Diseases, Nagoya University School of Medicine, Nagoya, Japan;*
[2]*Department of Pediatrics, Nagoya University Graduate School of Medicine, Nagoya, Japan and*
[3]*Department of Hematology and Oncology, Nagoya University Graduate School of Medicine, Nagoya, Japan*
E-mail: kiyoi@med.nagoya-u.ac.jp

References

1 Speck NA, Gilliland DG. Core-binding factors in haematopoiesis and leukaemia. *Nat Rev Cancer* 2002; **2**: 502–513.
2 Wechsler J, Greene M, McDevitt MA, Anastasi J, Karp JE, Le Beau MM *et al.* Acquired mutations in GATA1 in the megakaryoblastic leukemia of Down syndrome. *Nat Genet* 2002; **32**: 148–152.
3 Ahmed M, Sternberg A, Hall G, Thomas A, Smith O, O'Marcaigh A *et al.* Natural history of GATA1 mutations in Down syndrome. *Blood* 2004; **103**: 2480–2489.
4 Walters DK, Mercher T, Gu TL, O'Hare T, Tyner JW, Loriaux M *et al.* Activating alleles of JAK3 in acute megakaryoblastic leukemia. *Cancer Cell* 2006; **10**: 65–75.
5 Suzuki M, Abe A, Kiyoi H, Murata M, Ito Y, Shimada K *et al.* Mutations of N-RAS, FLT3 and p53 genes are not involved in the development of acute leukemia transformed from myeloproliferative diseases with JAK2 mutation. *Leukemia* 2006; **20**: 1168–1169.
6 Hirose Y, Kudo K, Kiyoi H, Hayashi Y, Naoe T, Kojima S. Comprehensive analysis of gene alterations in acute megakaryoblastic leukemia of Down's syndrome. *Leukemia* 2003; **17**: 2250–2252.
7 O'Shea JJ, Husa M, Li D, Hofmann SR, Watford W, Roberts JL *et al.* Jak3 and the pathogenesis of severe combined immunodeficiency. *Mol Immunol* 2004; **41**: 727–737.
8 Villeval JL, James C, Pisani DF, Casadevall N, Vainchenker W. New insights into the pathogenesis of JAK2 V617F-positive myeloproliferative disorders and consequences for the management of patients. *Semin Thromb Hemost* 2006; **32**: 341–351.